NWC TP 5880

Analysis of Harpoon Missile Structural Response to Aircraft Launches, Landings, Captive Flight and Gunfire

by
Allan G. Piersol
Bolt Beranek and Newman Inc.
for the
Engineering Department

JANUARY 1977

Naval Weapons Center
CHINA LAKE, CALIFORNIA 93555

Naval Weapons Center

AN ACTIVITY OF THE NAVAL MATERIAL COMMAND

R. G. Freeman, III, RAdm., USN ..... Commander
G. L. Hollingsworth ..... Technical Director

FOREWORD

This is a final report on the analysis of the Harpoon missile response to aircraft catapult launches, arrested landings, captive flight and gunfire. The work, authorized by AIRTASK A05P-204/2162/6000/00000 issued by the Naval Air Systems Command, was performed from May 1974 to January 1976. The information is released at the working level.

In the interest of economy and timeliness in presenting the information, the report is being published as originally submitted to NWC by the contractor, except for minor (typographical) changes to the text, formatting to NWC technical publication style, and preparation of the figures for reproduction.

Released by
B. W. Hays, *Head*
Engineering Department
1 July 1976

Under authority of
G. L. HOLLINGSWORTH
Technical Director

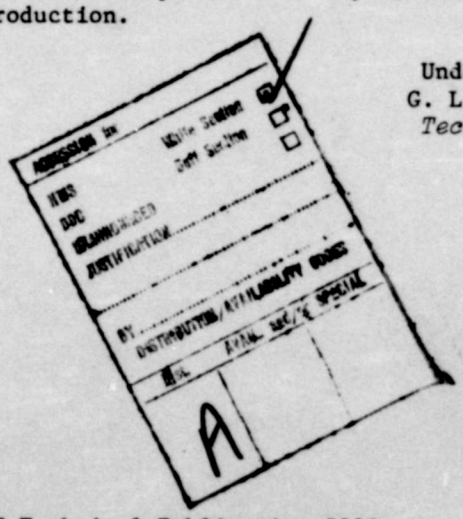

NWC Technical Publication 5880

Published by . . . . . .Technical Information Department
Collation . . . . . .Cover, 50 leaves
First printing . . . . . 205 unnumbered copies

UNCLASSIFIED

SECURITY CLASSIFICATION OF THIS PAGE (When Data Entered)

REPORT DOCUMENTATION PAGE

READ INSTRUCTIONS BEFORE COMPLETING FORM

1. REPORT NUMBER (13) NWC TP-5888	2. GOVT ACCESSION NO. (9)
3. RECIPIENT'S CATALOG NUMBER	
4. TITLE (and Subtitle) (6) Analysis of Harpoon Missile Structural Response to Aircraft Launches, Landings, Captive Flight and Gunfire.	5. TYPE OF REPORT & PERIOD COVERED Final rept. May 1974-Jan 1976.
6. PERFORMING ORG. REPORT NUMBER (14) BBN-3159	Project No. 137169
7. AUTHOR(s) (10) Allan G. Piersol, Bolt Beranek and Newman Inc.	8. CONTRACT OR GRANT NUMBER(s) (15) N60530-75-M-812C
9. PERFORMING ORGANIZATION NAME AND ADDRESS Bolt Beranek and Newman Inc. 21120 Vanowen Street Canago Park, CA 91303	10. PROGRAM ELEMENT, PROJECT, TASK AREA & WORK UNIT NUMBERS AIRTASK A05P-204/2162/6000/ 00000
11. CONTROLLING OFFICE NAME AND ADDRESS Naval Weapons Center China Lake, CA 93555 (12) 98p. (11)	12. REPORT DATE Jan 1977
	13. NUMBER OF PAGES 90
14. MONITORING AGENCY NAME & ADDRESS (if different from Controlling Office)	15. SECURITY CLASS. (of this report) Unclassified
	15a. DECLASSIFICATION/DOWNGRADING SCHEDULE

16. DISTRIBUTION STATEMENT (of this Report)

Approved for public release; distribution unlimited.

17. DISTRIBUTION STATEMENT (of the abstract entered in Block 20, if different from Report)

18. SUPPLEMENTARY NOTES

19. KEY WORDS (Continue on reverse side if necessary and identify by block number)

Harpoon Missile	Arrested Landings
Shock	Missile Structural Response
Vibration	Missile-Carrying Aircraft
Catapult Launches	Missile Response Measurements

20. ABSTRACT (Continue on reverse side if necessary and identify by block number)

See back of form.

(U) *Analysis of HARPOON Missile Structural Response to Aircraft Launches, Landings, Captive Flight and Gunfire*, by Allan G. Piersol, Bolt Beranek and Newman Inc. China Lake, Calif., Naval Weapons Center, January 1977. 90 pp. (NWC TP 5880, publication UNCLASSIFIED.)

(U) During its service life the HARPOON missile will be exposed to various types of shock and vibration loads which pose a reliability hazard to the missile and its equipment. This report discusses the response of the HARPOON missile to shock loads during catapult launches and arrested landings of the missile-carrying aircraft, long-term vibration during captive flight, and short-term vibration induced by aircraft gunfire. To evaluate the missile's response to these shock and vibration loads, a number of catapult launch and arrested landing tests were performed using an A-7E aircraft carrying an instrumented HARPOON missile; extensive captive flight vibration and surface pressure measurements were made for various flight conditions and carrying positions of the instrumented missile on A-7C, S-3A, and P-3C aircraft; and vibration caused by gunfire during the A-7C tests was measured.

(U) Although the primary purpose of this measurement program was to obtain HARPOON missile structural response data for comparison to the HARPOON environmental design criteria, also of interest was a comparison of the measured response levels to the test criteria of applicable specifications, as well as other available data for similar missiles.

TABLE OF CONTENTS

TABLE OF CONTENTS (Cont'd)

LIST OF FIGURES

LIST OF FIGURES (Cont'd)

LIST OF FIGURES (Cont'd)

LIST OF TABLES

LIST OF TABLES (Cont'd)

ANALYSIS OF HARPOON MISSILE STRUCTURAL RESPONSE TO AIRCRAFT LAUNCHES, LANDINGS, CAPTIVE FLIGHT AND GUNFIRE

1. INTRODUCTION

As for all externally carried aircraft stores, the HARPOON missile (AGM-84A) will be exposed during its service life to various types of shock and vibration loads which pose a reliability hazard to the missile and its equipment. The most significant of the shock and vibration environments directly associated with aircraft operations are the shock loads during catapult launches and arrested landings of the carriage aircraft, the long term vibration during captive flight, the short term vibration induced by aircraft gunfire, and the intense shock loads associated with flight launch ejections. The missile structural response to launch ejection shocks has been evaluated in an earlier report [1]. This study is concerned with the missile response to the other dynamic loads noted above.

To evaluate the missile response to the shock and vibration loads of interest, a number of catapult launch and arrested landing tests were performed at the U. S. Naval Air Test Center, Patuxent River, Maryland, using an A-7E aircraft carrying an

instrumented HARPOON missile. Extensive captive flight vibration and surface pressure measurements were made for various different flight conditions and carriage locations of the same instrumented missile on three different aircraft; an A-7C, an S-3A, and a P-3C. Limited amounts of vibration data during gunfire were measured during the A-7C tests.

The primary purpose of the measurement program was to provide data for assessing the structural response of the HARPOON missile as compared to the HARPOON environmental design criteria [2]. Also of interest, however, is a comparison of the measured response levels to the test criteria of applicable specifications, as well as other available data for similar missiles.

2. TEST CONFIGURATIONS AND INSTRUMENTATION

The HARPOON missile (AGM-84A) is a subsonic air breathing cruise missile designed for antiship applications. The layout of the missile is shown in Figure 1. The missile employes a low-level cruise trajectory, active radar guidance, and terminal maneuvering to assure maximum weapon effectiveness. During cruise, it is powered by a turbojet sustainer engine. HARPOON is designed for both air and surface launch, but the

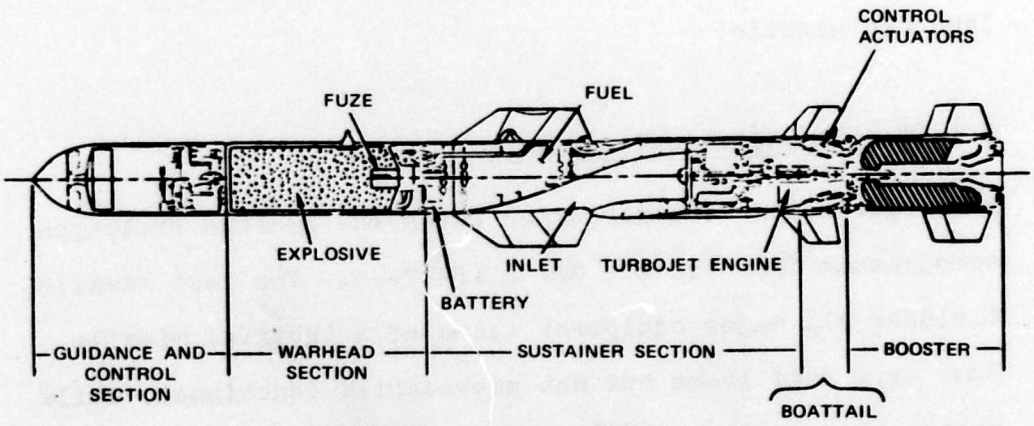

WING SPAN	36 IN.
DIAMETER	13.5 IN.
SHIPBOARD LENGTH	180 IN.
SHIPBOARD WEIGHT	1,470 LB
AIR LAUNCH LENGTH	151 IN.
AIR LAUNCH WEIGHT	1,150 LB

FIGURE 1. Diagram of the HARPOON Missile.

tests reported herein are concerned only with the air launched missile.

2.1 Test Missile Configuration

All experiments were performed using the HARPOON Prototype Aerodynamic Test Vehicle No. 2 (PATV-2). The test missile included all major equipment items of a tactical missile. Some were real items but not necessarily functional, while others were dummy loads simulating the mass and center of gravity of the item being represented. Water was used to simulate the fuel. No attempt was made to simulate wire bundles, valves, tubing or other plumbing components; nor was secondary structure included except as required to mount equipment. Nevertheless, the test missile provided a reasonably accurate simulation of a tactical missile in size, weight and center of gravity, as summarized in Table 1.

Table 1. Weight and C. G. Characteristics for Typical HARPOON Tactical Missile

Item	Weight (lbs)	C.G. Location (Station No.)
Radome Section	4.60	18.50
Seeker	80.52	26.08
Guidance Wheel	46.26	39.16
Guidance Structure	17.03	35.12
T & E Section (Warhead)	519.91	62.56
Tank Section	139.02	103.84
Engine Section	131.25	142.70
Boattail	71.35	155.37
Wings	60.69	100.34
Fuel	107.51	105.81
Total	1178.14	83.89

2.2 Data Transducers

Eleven structural acceleration measurements and three surface pressure measurements were made at various locations on the test missile, as illustrated in Figure 2 and detailed in Table 2. The acceleration measurements were made using Gulton piezoelectric crystal accelerometers in conjunction with Gulton charge amplifiers. The surface pressure measurements were made using Gulton flush mounted pressure transducers in conjunction with Gulton charge amplifiers. All transducers and amplifiers were procured against special McDonnell-Douglas specifications. The frequency response was 10 to 2,000 Hz in all cases.

Referring to Figure 2 and Table 2, six of the accelerometers were mounted internally on primary structure near the mounting points of the seeker and midcourse guidance unit (MGU). Hence, these measurements should provide a good indication of the input shock and vibration to these two critical equipment items. Three other accelerometers were mounted near the forward hook to help define those loads introduced to the missile through the aircraft interface (principally the shock loads during catapult launches and arrested landings). The final two accelerometers were located in the engine section to provide a measure of the input shock and vibration to the engine. Two

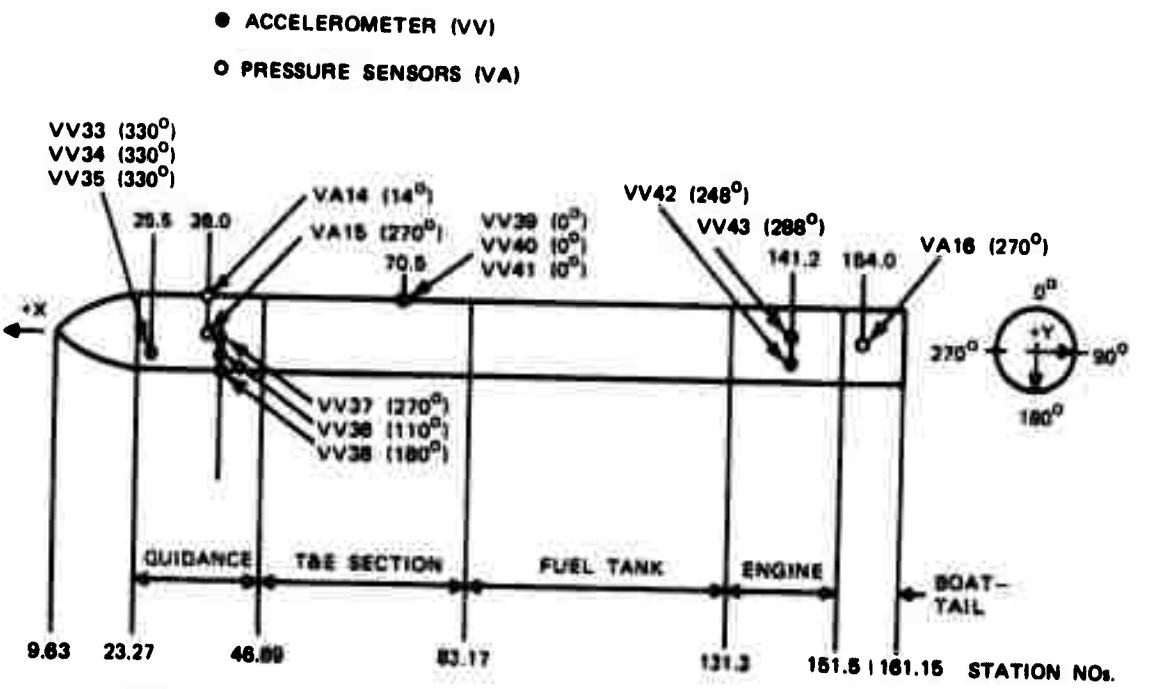

FIGURE 2. Diagram of Transducers Locations for HARPOON Missile Tests.

Table 2. Summary of Transducer Locations for HARPOON Missile Tests

No.	Type	Location	Direction	Sta. No.
VA 14	pressure	guidance section surface	radial	36.0, 14°
VA 15	pressure	guidance section surface	radial	36.0, 270°
VA 16	pressure	boattail surface	radial	154.0, 270°
VV 33	acceleration	seeker bulkhead	axial (x)	25.5, 330°
VV 34	acceleration	seeker bulkhead	lateral (y)	25.5, 330°
VV 35	acceleration	seeker bulkhead	vertical(z)	25.5, 330°
VV 36	acceleration	MGU mounting structure	axial (x)	38.6, 110°
VV 37	acceleration	MGU mounting structure	lateral (y)	38.6, 270°
VV 38	acceleration	MGU mounting structure	vertical(z)	38.6, 180°
VV 39	acceleration	fwd. aircraft hook	axial (x)	70.5, 0°
VV 40	acceleration	fwd. aircraft hook	lateral (y)	70.5, 0°
VV 41	acceleration	fwd. aircraft hook	vertical(z)	70.5, 0°
VV 42	acceleration	engine wall	radial	141.2, 248°
VV 43	acceleration	engine wall	axial (x)	141.2, 288°

of the pressure transducers were flush mounted near the top and on the side of the guidance section to measure the aeroacoustic excitation of the missile in the region of critical equipment items during captive flight. The third pressure transducer was mounted on the side of the boattail where the aeroacoustic loads during captive flight should be most severe.

2.3 Data Transmission and Recording

All signals from the data transducers were transmitted to a ground station using a PAM FM/FM telemetry system. The system consisted of a high level main multiplexer and a hybrid (high and low level) submultiplexer mixed with the output of three subcarrier oscillators (SCO's). The telemetry R.F. link was comprised of a 4 watt S-band transmitter and a wrap-around omnidirectional antenna. Three SCO channels were used for transmission of the 11 structural vibration measurements and the 3 acoustic measurements. An encoder (electronic stepper switch) activated within the parent aircraft was employed to select a combination of parameters to be processed via the SCO's. The ground station recorder was an Ampex FR 1800.

3. TEST PROCEDURES

A number of catapult launch, arrested landing, and captive flight tests were performed to acquire the desired data using the following procedures.

3.1 Procedures for Catapult Launch Tests

The shock response of the HARPOON missile to catapult launches of the carriage aircraft was measured by mounting the instrumented test missile on an A-7E aircraft (No. 157456), and performing test launches of the aircraft from the NATC simulated catapult launch and arrested landing facility at Patuxent River, Maryland. Missile response data were recorded during four trial launches from a C-7 catapult, as summarized in Table 3. Only three channels of acceleration data could be recorded during any given launch. Hence, four launches were required to record the signals from all eleven accelerometer locations.

For all four launches, the test missile was mounted at weapon station location No. 1. This is the furthest outboard wing station on the port side of the A-7E aircraft, as illustrated in Figure 3(c). The tests were performed with the missile at this station because it was believed that the dynamic response of the aircraft to the catapult launches would be most severe at this location.

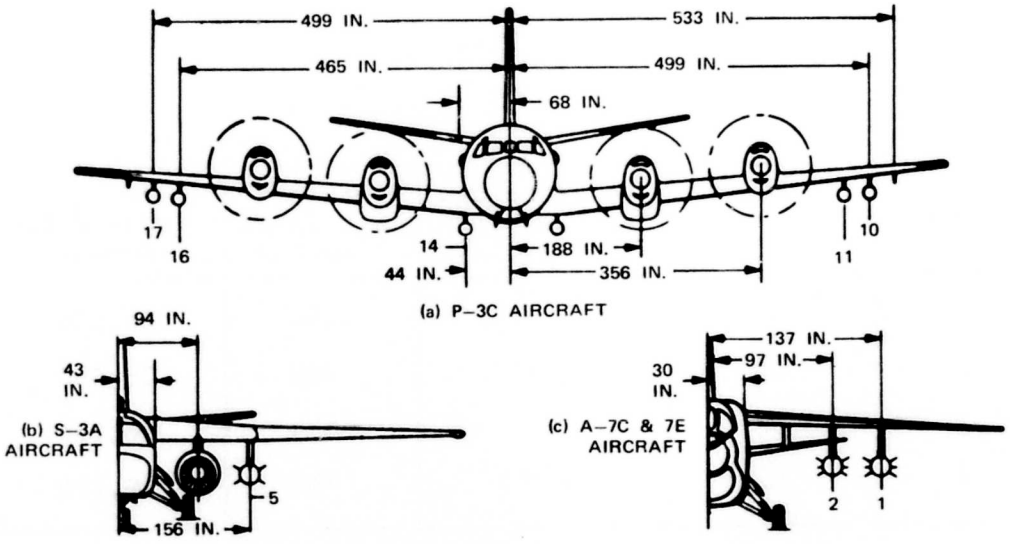

FIGURE 3. Weapon Station Locations on Aircraft Used For HARPOON Missile Tests.

Table 3. Summary of Test Launches of A-7E Aircraft With HARPOON missile on Station No. 1.

Launch No.*	Distance Off Center (inches)	Longitudinal Acceleration (g)	Launch End Speed (knots)	Aircraft Gross Weight (pounds)
1	0	5.3	160	26,100
2	6L	5.6	168	25,400
3	0	6.0	174	26,000
4	0	4.7	150	25,700

*All launches were performed using C-7 catapult.

3.2 Procedures for Arrested Landing Tests

The shock response of the HARPOON missile to arrested landings of the carriage aircraft was measured using the same missile-aircraft configuration and test facility employed for the catapult launch tests. Missile response data were recorded during ten trial arrested landings using a MK-7 Mod 3 arresting gear, as summarized in Table 4. Note that the trial landings were performed over a wide range of aircraft sink rates. However, the maximum sink rate achieved was about 19 ft/sec, well below the design limit of 26 ft/sec for this aircraft.

Table 4. Summary of Test Arrested Landings of A-7E Aircraft With HARPOON Missile on Station No. 1.

Landing No.*	Distance Off Center (feet)	Longitudinal Acceleration (g)	Sink Rate LMG/RMG ** (ft./sec.)	Engaging Speed (knots)	Aircraft Gross Wt. (pounds)
1	11L	3.2	14.9/14.0	129	24,900
2	0	3.2	16.0/15.5	131	24,500
3	8L	3.2	17.9/18/5	132	24,000
4	5L	3.2	15.9/16/4	134	25,100
5	6L	3.2	18.8/19.1	133	24,700
6	17L	3.2	9.9/9.2	136	24,400
7	11R	3.3	8.2/8.9	131	24,000
8	8L	3.6	2.3/2.4	132	25,000
9	3L	4.2	10.4/10.7	143	24,900
10	3L	4.3	12.6/12.6	150	24,400

* All landings were performed using a MK-7 Mod 3 arresting gear.

** Left Main Gear/Right Main Gear

3.3 Procedures For Captive Flight Tests

The vibration response of the HARPOON missile during captive flight was measured with the instrumented test missile mounted at various weapon stations on three different carriage aircraft; a P-3C (No. 6512), an S-3A (No. 992), and an A-7C (No. 156776). Vibration and pressure data were recorded for a wide range of flight conditions, as summarized in Table 5. The various weapon station locations of the test missile are illustrated in Figure 3.

The three aircraft used for the captive flight tests represent a good cross-section of the type of aircraft which might carry the HARPOON missile on tactical missions. The P-3C (Orion) is a four engine propeller driven patrol aircraft with a top speed of about 400 knots. One should expect the vibration environment of the HARPOON missile on this aircraft to include strong periodic contributions from the propeller generated noise. The S-3A (Viking) is an anti-submarine aircraft powered by two wind mounted jet engines. The HARPOON vibration environment on this aircraft would probably include jet noise contributions. The A-7C (Corsair 2) is a subsonic attack aircraft powered by a single fuselage enclosed jet engine, and is capable of flight at dynamic pressures in

Table 5. Summary of Captive Flight Conditions for HARPOON Missile on Various Aircraft

Aircraft	Weapon Station	Flight Condition	Calibrated Airspeed (knots)	Altitude (feet)	Mach No.	Dynamic Pressure (psf)
P-3C	10	Take-off	--	--	--	--
		Level Flight	355	1000	0.55	427
			275	1000	0.42	257
			140	1000	0.22	66
			350	3000	0.56	416
			210	3000	0.34	150
			305	15000	0.61	305
			255	25000	0.62	210
		Level Flight	140	25000	0.35	66
		2g turn	260	5000	0.42	226
	10	V_{max} Dive	355*	7000*	0.60	421*
	14	Take-off	--	--	--	--
		Level Flight	380	1000	0.59	490
			275	1000	0.42	257
			140	1000	0.22	66
			340	3000	0.54	392
			210	3000	0.34	150
			305	15000	0.61	305
			255	25000	0.62	210
		Level Flight	140	25000	0.35	66
		2g	270	5000	0.45	246
P-3C	14	V_{max} Dive	355*	7000*	0.60	421*
S-3A	5	Take-off	--	--	--	--
		Level Flight	340	1000	0.52	392
			270	1000	0.42	257
			140	1000	0.22	66
			340	3000	0.54	392
			314	15000	0.62	326
		Level Flight	260	25000	0.63	219
S-3A	5	3.5g Turn	320	12000	0.60	340

Table 5. Summary of Captive Flight Conditions for HARPOON Missile on Various Aircraft (Cont'd)

Aircraft	Weapon Station	Flight Condition	Calibrated Airspeed (knots)	Altitude (feet)	Mach No.	Dynamic Pressure (psf)
A-7C	1	Take-off	--	--	--	--
		Level Flight	550	1000	0.85	1026
			350	1000	0.54	416
			180	1000	0.28	110
			430	12000	0.80	595
			200	12000	0.38	137
			450	15000	0.87	636
			410	15000	0.80	532
			340	30000	0.89	352
			300	30000	0.80	281
		Level Flight	190	30000	0.52	117
	1	5.5g Turn	450	1000	0.69	716
	2	Take-off	--	--	--	--
		Level Flight	495	2500	0.78	831
			350	2500	0.55	416
			195	2500	0.31	129
			440	8000	0.76	636
			440	15000	0.86	610
			340	29000	0.88	354
			300	29000	0.78	279
		Level Flight	195	29000	0.52	125
		5.5g Turn	450	1000	0.69	716
A-7C	2	V_{max} Dive	550*	11000*	0.98*	958*

*Average value over record length of measurement

excess of 1000 psf. Hence, the missile environment in this case should be dominated at extreme flight conditions by aerodynamic excitation.

3.4 Procedures For Gunfire Tests

The vibration response of the HARPOON missile during gunfire of the carriage aircraft was measured with the instrumented test missile mounted on weapon station location No. 2 of the same A-7C aircraft used for the captive flight tests. The aircraft was equipped with an internally mounted M61A1 20 mm Gatling gun. During level flight at 1000 ft with a flight dynamic pressure of q = 700 psf, several bursts of 500 rounds each were fired, some with a firing rate of 4000 rounds/minute and others with a rate of 6000 rounds/minute. Vibration and surface pressure data were recorded just prior to the gunfire bursts and then during the bursts.

4. DATA ANALYSIS PROCEDURES

All data from the various HARPOON missile tests were processed and analyzed at NATC, Patuxent River, Maryland. The acceleration and pressure records were reduced to peak levels, shock spectra, and/or power spectra, depending upon the types of measurements, as will now be summarized.

4.1 Catapult Launch and Arrested Landing Data

The transient signals from the eleven accelerometers recorded during each of the catapult launch and arrested landing tests were plotted out as time histories using an oscillograph, and the peak acceleration value of each time history was tabulated. Selected records were then reduced to maximax response (shock) spectra over the frequency range from 2 to 2000 Hz using a Spectral Dynamics SD-320 shock spectrum analyzer. The shock spectra were computed for two damping factors; $\zeta = 0.05$ ($Q = 10$) and $\zeta = 0.01$ ($Q = 50$). The applications and interpretations of shock spectra for transient missile response environments have been reviewed and discussed in the report covering the HARPOON launch ejection shock [1] and, hence, need not be pursued here. More general discussions of the measurement and interpretation of shock spectra data are available from the open literature [3,4].

4.2 Captive Flight Vibration and Pressure Data

The signals from the eleven accelerometers and three surface pressure transducers recorded during the captive flight tests were reduced to rms values using a calibrated voltmeter, and to power (auto) spectral density functions using a Federal

Scientific UA-6A Ubiquitos spectrum analyzer in conjunction with Federal Scientific 129B digital averager. The auto-spectra were computed over a frequency range from 10 to 2000 Hz with a nominal resolution bandwidth of B = 10 Hz and an averaging time of T = 6.4 seconds, providing estimates with n = 2BT = 128 degrees-of-freedom. Hence, the resulting spectral density estimates have a coefficient of variation (normalized standard deviation) of ε = 12.5%. It follows that a 95% confidence interval for the spectral density value at any frequency in the analyzed data is approximately $\pm$ 1 dB. Details on the applications and interpretations of spectral density functions are available from the open literature [5,6].

4.3 Gunfire Vibration and Pressure Data

The signals from six forward accelerometers in the seeker and guidance section as well as the three surface pressure transducers recorded just prior to and during the bursts of 20 mm. gunfire were reduced to rms values using a calibrated voltmeter, and to power spectral density functions using the Federal Scientific Ubiquitos analyzer. For the measurements prior to the bursts of gunfire, the power spectra were computed over a frequency range from 10 to 2000 Hz with a nominal resolution bandwidth of B = 10 Hz and an averaging time of either T = 3.2 or T = 6.4 secs, giving n = 2BT = 64 or

128 degrees-of-freedom, respectively. N = 128 degrees-of-freedom provides an estimate with a 95% confidence interval of about ± 1 dB, while n = 64 degrees-of-freedom yields a confidence interval of approximately ± 1.5 dB.

For the measurements during the bursts of gunfire, the autospectra were computed over a frequency range from 40 to 2000 Hz with a nominal resolution bandwidth of B = 40 Hz. The averaging time was selected to correspond to a period when the gunfire was relatively stable. This varied from 0.4 secs to 1.8 secs. At the lower limit of T = 0.4 secs, the degrees-of-freedom for the estimates are n = 32 corresponding to a 95% confidence interval of about - 2.5 dB to + 2 dB.

5. TEST RESULTS

The basic results of the tests consist of acceleration time histories, peak acceleration values, shock spectra of acceleration transients, and power spectra of stationary acceleration and pressure signals. The pertinent characteristics of these results are now summarized for the various tests.

5.1 Catapult Launch Tests

Typical time histories of the acceleration response measured

on the HARPOON structure at the forward hook (VV39-41) during a catapult launch are shown in Figure 4. Note that the time histories display two distinct transient events separated in time by about two seconds. The first event corresponds to the start of the launch when the catapult load is initially applied to the aircraft, and the second corresponds to the end of the launch when separation occurs. The separation transient is generally more severe than the launch initiation transient, suggesting that the separation load occurs more abruptly than the launch initiation load. In both cases, however, the transients display a distinct oscillatory character at about 10 Hz.

The peak acceleration levels measured at the eleven accelerometer locations on the HARPOON structure during the various catapult launches are summarized in Table 6. The peak accelerations are shown separately for the launch initiation and separation transients. Note that the peak accelerations in any given direction do not vary dramatically with location.

A typical shock spectrum of the HARPOON response to the catapult launch load is shown in Figure 5. This spectrum, computed for both Q = 10 and Q = 50, is for the vertical acceleration transient measured at the forward hook, as

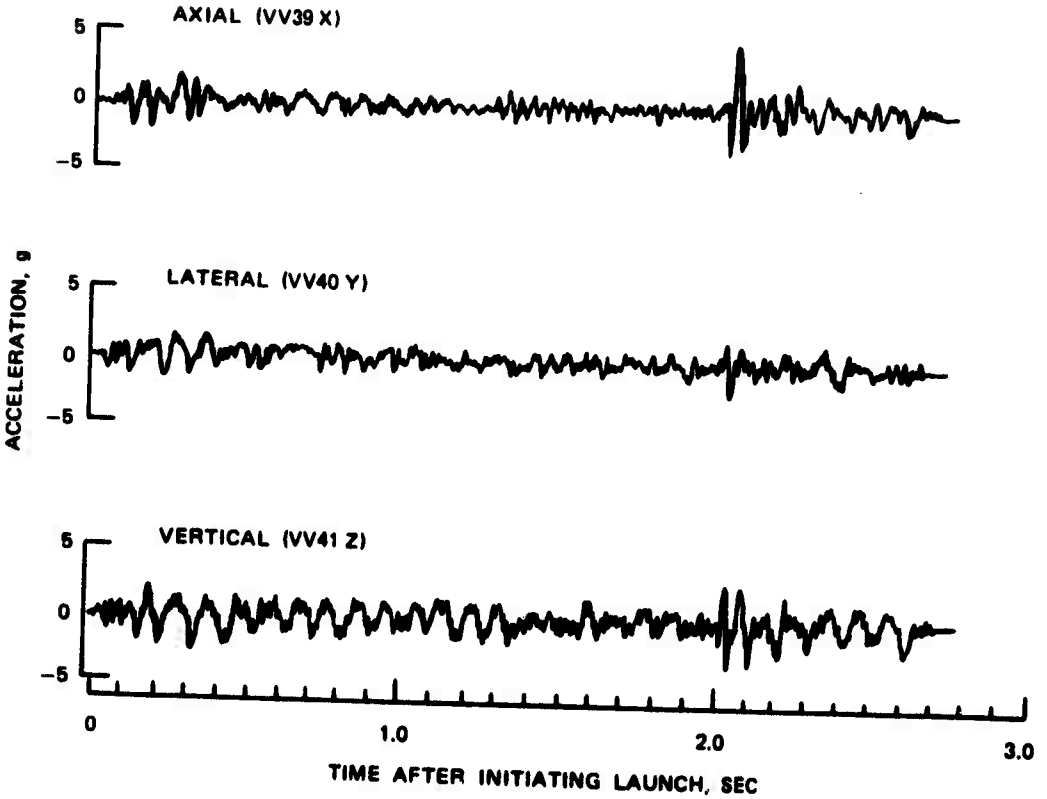

FIGURE 4. Time Histories of HARPOON Missile Acceleration Response at Forward Hook During Catapult Launch of A-7E Aircraft.

Table 6. Summary of Peak Acceleration Levels on HARPOON Structure During Catapult Launches of A-7E Aircraft

Measurement Location		Direction	Launch No.*	Max Launch Accel., g	Peak Missile Response Acceleration, g	
No.	Description				Initiation	Separation
VV 33	Seeker bulkhead	Axial	2	5.6	1.5	4.0
VV 34		Lateral	2	5.6	1.3	3.3
VV 35		Vertical	2	5.6	3.8	6.3
VV 36	MGU mounting structure	Axial	1	5.3	1.8	4.8
VV 37		Lateral	1	5.3	1.3	1.3
VV 38		Vertical	1	5.3	3.5	4.8
VV 39	Forward aircraft hook	Axial	3	6.0	1.3	4.0
VV 40		Lateral	3	6.0	--	1.3
VV 41		Vertical	3	6.0	2.0	2.5
VV 42	Engine wall	Radial	4	4.7	2.0	4.5
VV 43		Vertical	4	4.7	1.3	2.8

*See Table 3 for details.

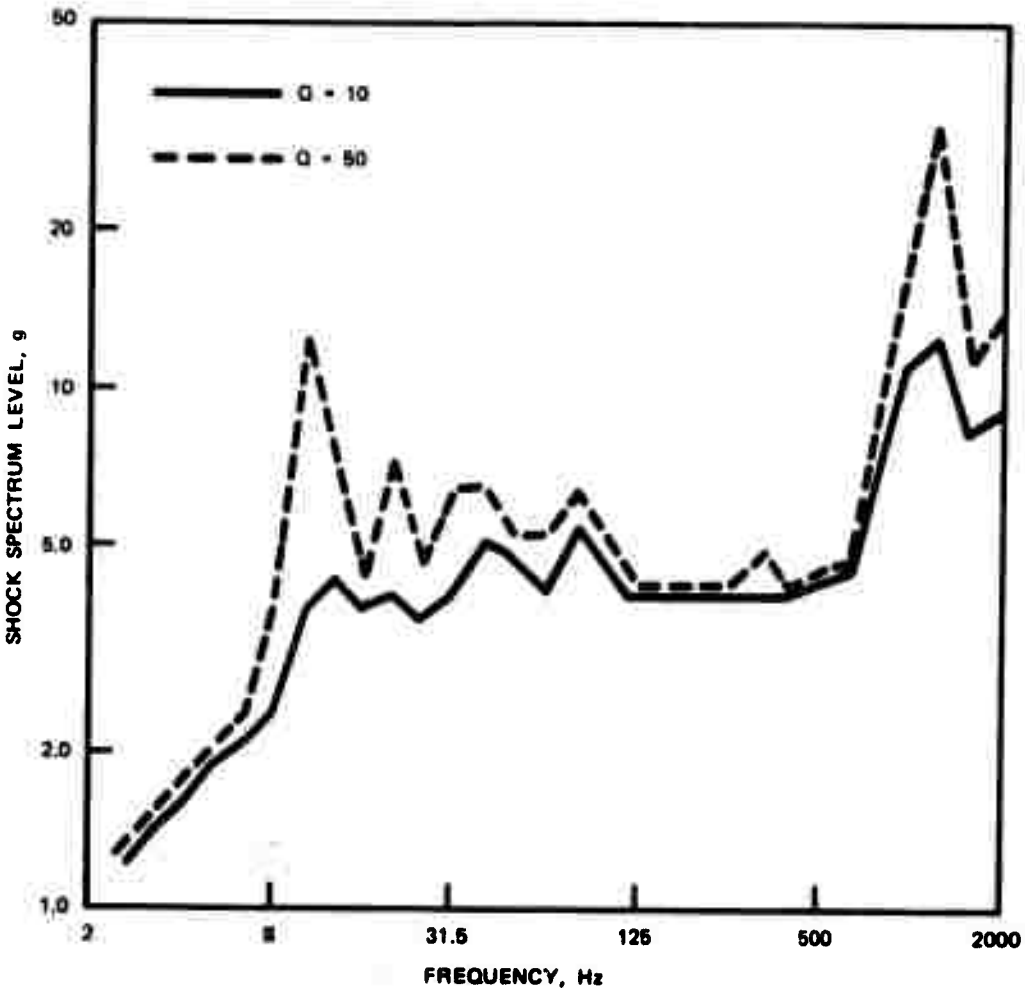

FIGURE 5. Shock Spectrum of HARPOON Vertical Response at the Forward Hook During Catapult Launch of A-7E Aircraft.

previously presented in Figure 4(c). Note that this is a maximax shock spectrum for the total launch transient, including both the initiation and separation events. Shock spectra were also computed for the initiation and separation events separately. Such data are illustrated for the vertical acceleration input to the MGU (VV 38) in Figure 6. The shock spectra in this figure were computed using Q = 10. Note that the spectral values for the separation pulse are somewhat higher at most frequencies than the values for the initiation pulse. Referring to Table 6, this is consistent with the fact that the separation pulse displayed a higher peak acceleration level. The shock spectrum for the overall transient approximately envelops the shock spectra for the individual events.

The shock spectra shown in Figures 5 and 6, as well as the spectra measured at all other locations during the catapult launch tests, have certain common characteristics. Specifically, at the lower frequencies, they rise to a maximum or near maximum value at about 10 Hz. Referring to the typical time histories in Figure 4, this is consistent with the fact that the transient has a distinct oscillatory character at about 10 Hz, probably representing the elastic mode of the A-7E-HARPOON combination. At the higher frequencies, the spectra tend to rise to a second peak at about 1k Hz, which may be

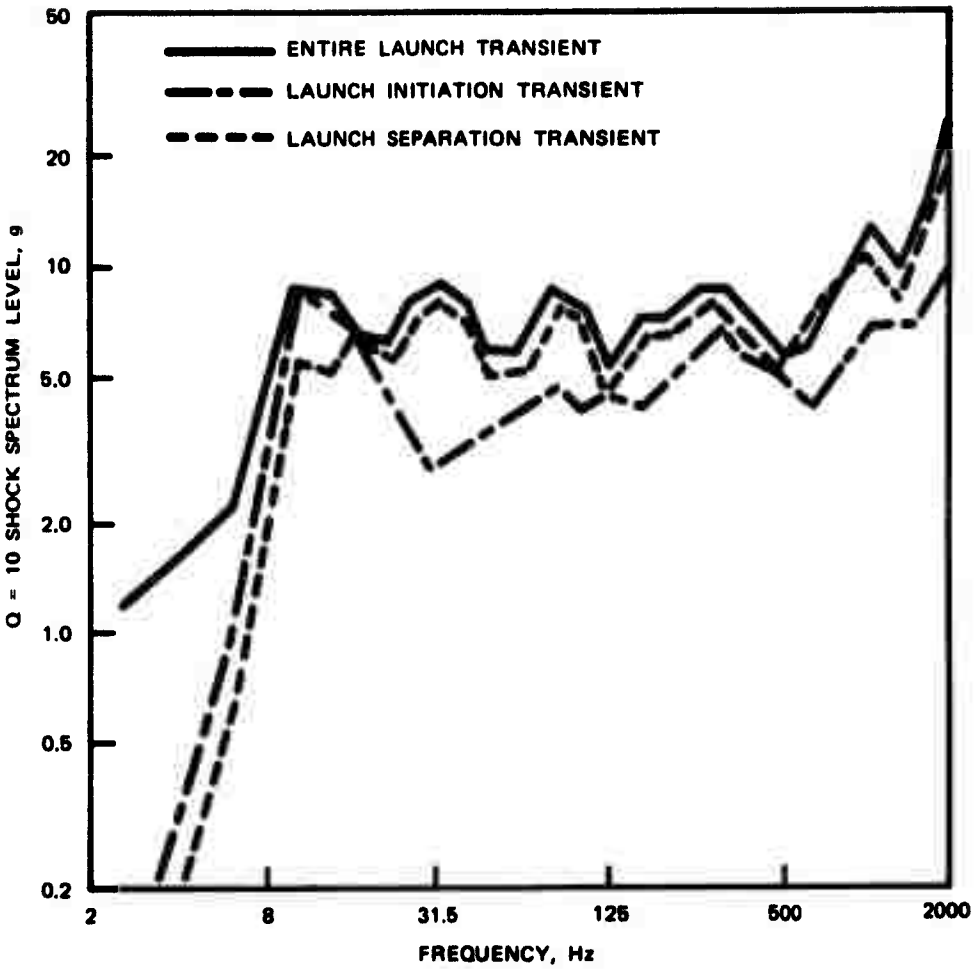

FIGURE 6. Q=10 Shock Spectra of HARPOON Vertical Response at the MGU During Different Phases of Catapult Launch of A-7E Aircraft.

related to the first flexural ring mode of the HARPOON missile shell.

5.2 Arrested Landing Tests

Typical time histories of the acceleration response measured on the HARPOON structure at the forward hook (VV 39-41) during an arrested landing are shown in Figure 7. Unlike the catapult launch data, the time histories in this case reveal only one distinct transient event. However, the transient has the same general oscillatory character at about the same frequency, namely, 10 Hz.

The peak acceleration levels measured at the eleven accelerometer locations on the HARPOON structure during the various arrested landings are summarized in Table 7. As for the catapult launch data, the arrested landing acceleration levels in any given direction do not vary dramatically with location on the missile. Furthermore, the acceleration levels at a given location are relatively insensitive to the aircraft sink rate at landing. For example, the peak vertical acceleration recorded at the forward hook (VV 41) for a landing with a sink rate of 19 ft./sec. is only about twice the peak acceleration at this location for a landing with a sink rate of 2.4 ft./sec. Finally, comparing the results in Tables 6 and 7,

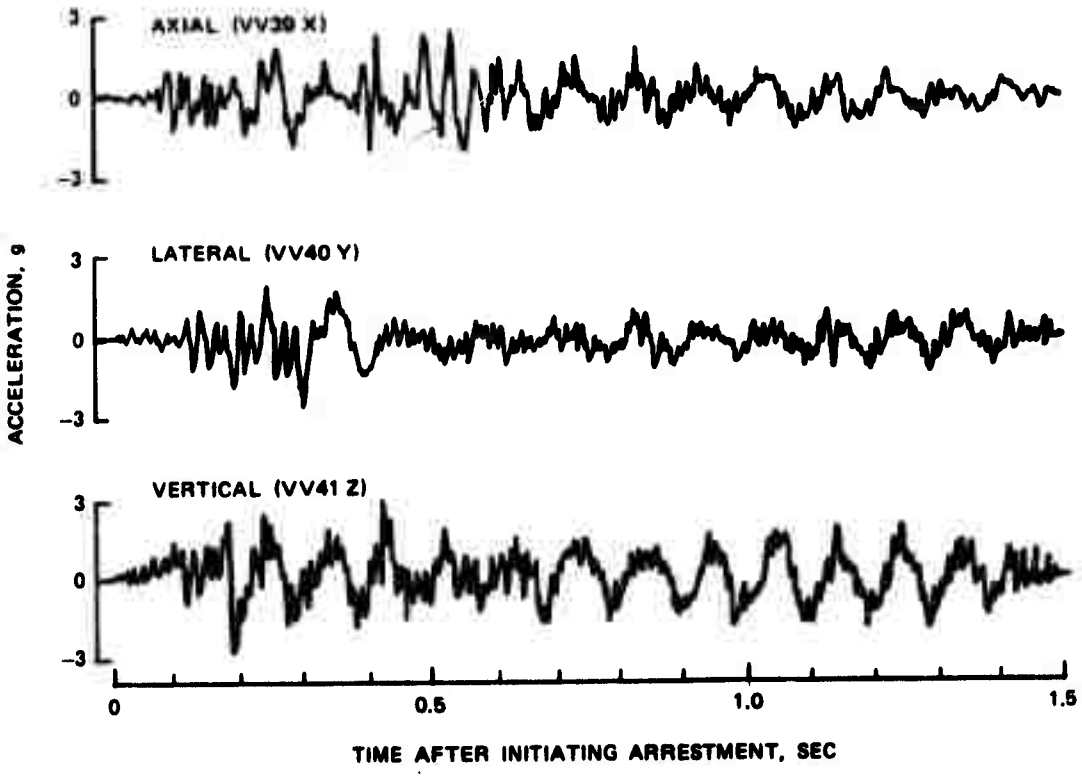

FIGURE 7. Time Histories of HARPOON Missile Acceleration Response at Forward Hook During Arrested Landing of A-7E Aircraft.

Table 7. Summary of Peak Acceleration Levels on HARPOON Structure During Arrested Landings of A-7E Aircraft

Measurement Location Description	No.	Direction	Arrested Landing No.	Sink Rate* (ft./sec.)	Max. Decel.,g	Peak Missile Response Acceleration (g)
Seeker Bulkhead	VV 33	Axial	1	14.5	3.2	3.5
	VV 34	Lateral	1	14.5	3.2	3.3
	VV 35	Vertical	1	14.5	3.2	3.8
MGU Mounting Structure	VV 36	Axial	9	10.6	4.2	4.8
			10	12.6	4.3	2.5
	VV 37	Lateral	9	10.6	4.2	2.0
			10	12.6	4.3	1.3
	VV 38	Vertical	6	9.6	3.2	3.8
			9	10.6	4.2	5.0
			10	12.6	4.3	2.5
Forward Aircraft Hook	VV 39	Axial	2	15.8	3.2	2.8
			3	18.2	3.2	2.5
			4	16.2	3.2	2.3
			5	19.0	3.2	3.0
			8	2.4	3.6	2.5
	VV 40	Lateral	2	15.8	3.2	2.5
			3	18.2	3.2	1.5
			4	16.2	3.2	1.8
			5	19.0	3.2	2.0
			8	2.4	3.6	1.3
	VV 41	Vertical	2	15.8	3.2	2.5
			3	18.2	3.2	2.5
			4	16.2	3.2	2.5
			5	19.0	3.2	2.5
			8	2.4	3.6	1.3
Engine Wall	VV 42	Radial	6	9.6	3.2	5.0
	VV 43	Vertical	6	9.6	3.2	2.3

*Average sink rate; see Table 4 for details.

it is seen that the peak missile response accelerations measured during the arrested landings are not significantly different, on the average, from the levels measured during the catapult launches.

Now concerning the shock spectra of the arrested landing transients, the maximax shock spectra of the acceleration transients recorded at most locations are similar in character and level to the shock spectra of the transients recorded during the catapult launches. This fact is illustrated in Figure 8, which presents the shock spectrum of the vertical acceleration measured at the forward hook (VV 41) for an arrested landing with a sink rate of 18.2 (Landing No. 3). Comparing these data to the spectra computed at the same location for the catapult launch transient in Figure 5, it is seen that the spectra levels are quite similar at all but the lowest frequencies for both the Q = 10 and Q = 50 results. At frequencies below 3 Hz, the catapult launch levels are somewhat higher. This is obviously due to the fact that the catapult launches involved two distinct transient events separated in time by about 2 seconds, producing a contribution to the shock spectrum at very low frequencies.

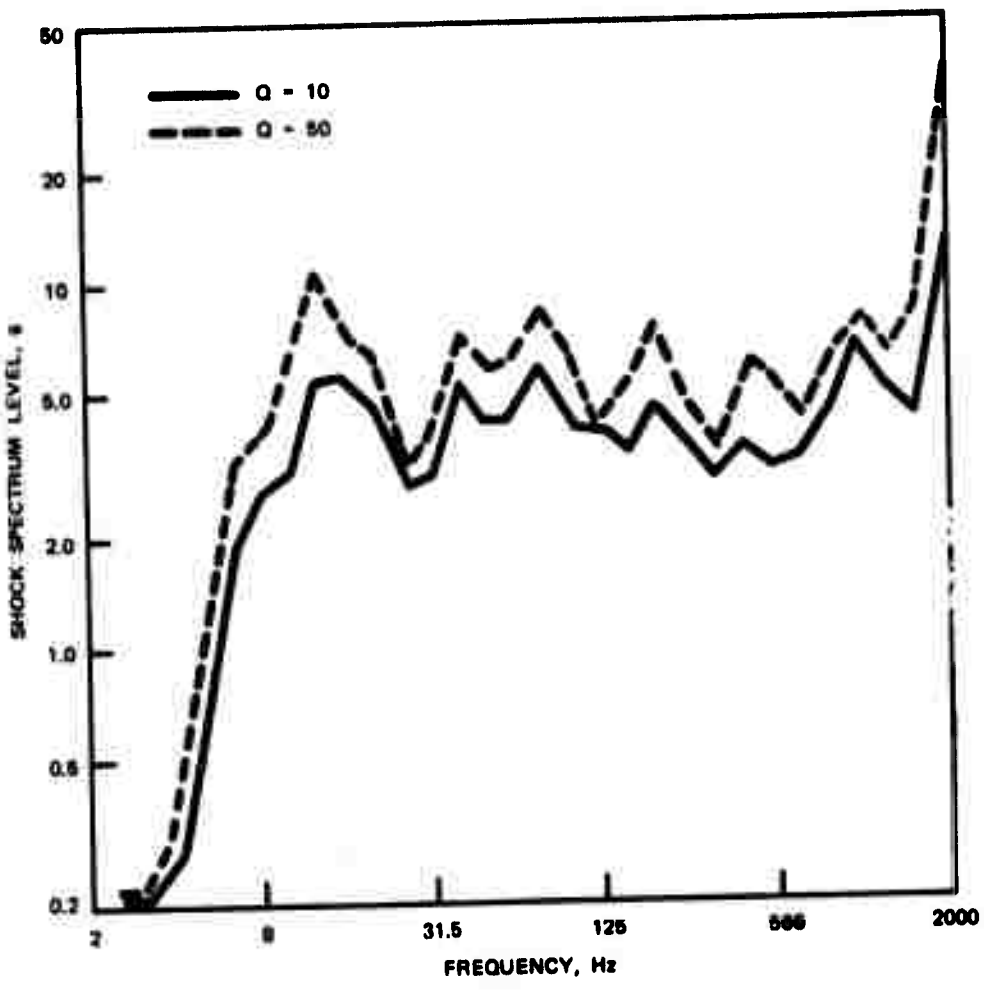

FIGURE 8. Shock Spectrum of HARPOON Vertical Response at the Forward Hook During Arrested Landing of A-7E Carriage Aircraft.

5.3 Captive Flight Tests

The rms vibration levels measured at the eleven accelerometer locations on the HARPOON missile structure during captive flight of the three test aircraft are summarized for various flight conditions in Table 8. The rms values of the fluctuating surface pressure levels measured by the three flush mounted pressure transducers are shown in Table 9. Note that both the vibration and pressure levels generally increase with increasing dynamic pressure, as would be expected for an externally carried aircraft store in captive flight [7,8]. Further note that the maximum levels usually occur near the aft end of the missile (Locations VV 42, VV 43, and VA 16). This is also consistent with past measurements of captive flight vibration and surface pressure environments for externally carried aircraft stores [7].

The power spectra of the recorded captive flight vibration measurements are highly "peaked" and generally cover a wide dynamic range, as is characteristic of spectra for structural vibration response data. The spectra differ substantially from one location to another on a given aircraft, but are reasonably similar at a given location and flight condition from one aircraft to another. This is demonstrated in Figure 9, which presents the power spectra of the vertical vibration

Table 8. Summary RMS Vibration Levels on HARPOON Structure During Captive Flight On Various Aircraft

Aircraft	Wpn Sta.	Flight Condition: Altitude (kft)	Air-speed (kts)	Mach No.	Dyn. Pressure (psf)	Overall rms Vibration Level in g For Various Locations: Seeker Bulkhead Axial VV33	Seeker Bulkhead Lat. VV34	Seeker Bulkhead Vert. VV35	MGU Mounting Axial VV36	MGU Mounting Lat. VV37	MGU Mounting Vert. VV38	Forward Hook Axial VV39	Forward Hook Lat. VV40	Forward Hook Vert. VV41	Engine Rad. VV42	Engine Axial VV43
P-3C	10	0	0	0	0	---	---	---	0.28	0.18	0.32	---	---	---	---	---
		1	140	0.22	66	0.11	0.18	0.07	0.07	0.07	0.07	0.07	0.07	0.07	0.28	0.14
		1	275	0.42	257	0.28	0.67	0.35	0.35	0.18	0.21	0.11	0.21	0.14	1.40	0.35
		1	355	0.55	427	0.53	1.11	0.78	0.71	0.39	0.50	0.25	0.53	0.39	2.40	0.71
		3	210	0.34	150	0.14	0.31	0.14	0.14	0.07	0.18	0.11	0.14	0.14	0.51	0.28
		3	350	0.56	416	0.64	1.10	0.78	0.78	0.35	0.42	0.25	0.53	0.39	2.12	0.64
		15	305	0.61	305	0.42	1.13	0.60	0.64	0.35	0.38	0.21	0.53	0.35	1.84	0.57
		25	140	0.35	66	0.14	0.22	0.21	0.11	0.07	0.14	0.11	0.28	0.11	0.42	0.14
	10	25	255	0.62	210	0.35	0.67	0.42	0.49	0.28	0.25	0.18	0.28	0.25	0.99	0.28
	14	0	0	0	0	---	---	---	---	---	0.32	---	---	---	0.40	0.20
		1	140	0.22	66	0.07	0.13	0.11	0.11	0.11	0.11	0.07	0.11	0.11	0.30	0.14
		1	275	0.42	257	0.25	0.58	0.32	0.28	0.18	0.21	0.11	0.21	0.21	1.00	0.28
		1	380	0.59	490	0.39	0.85	0.42	0.50	0.35	0.39	0.14	0.35	0.35	1.80	0.57
		3	210	0.34	150	0.11	0.18	0.14	0.18	0.11	0.14	0.07	0.11	0.11	0.40	0.21
		3	340	0.54	392	0.35	0.89	0.42	0.57	0.39	0.42	0.25	0.50	0.46	2.00	0.49
		15	305	0.61	305	0.32	0.71	0.35	0.46	0.28	0.32	0.18	0.35	0.35	1.70	0.49
		25	140	0.35	66	0.11	0.13	0.25	0.11	0.11	0.14	0.07	0.11	0.14	0.40	0.21
P-3C	14	25	255	0.62	210	0.32	0.53	0.32	0.42	0.35	0.35	0.14	0.28	0.25	1.40	0.35
S-3A	5	1	140	0.22	66	0.07	0.07	0.07	0.07	0.07	0.07	---	---	---	---	---
		1	275	0.42	257	0.21	0.53	0.21	0.25	0.14	0.14	0.07	0.18	0.14	0.85	0.21
		1	340	0.52	392	0.35	0.89	0.35	0.42	0.28	0.35	0.18	0.32	0.28	1.70	0.49
		3	340	0.54	392	0.39	0.81	0.35	0.35	0.25	0.21	0.18	0.35	0.25	1.84	0.49
		3	340	0.54	392	0.42	0.96	0.35	0.35	0.21	0.21	0.11	0.35	0.25	1.98	0.49
		15	314	0.62	326	0.28	0.81	0.35	0.42	0.21	0.28	0.11	0.32	0.25	1.56	0.42
S-3A	5	25	260	0.63	219	0.18	0.50	0.18	0.35	0.18	0.18	0.07	0.18	0.14	0.85	0.28
A-7C	1	0	0	0	0	0.11	0.25	0.11	---	---	---	---	---	---	---	---
		1	180	0.28	110	0.14	0.25	0.18	0.11	0.11	0.11	0.07	0.11	0.11	0.42	0.21
		1	350	0.54	416	0.25	0.53	0.28	0.32	0.21	0.25	0.14	0.21	0.25	1.27	0.42
		1	550	0.85	1026	0.71	1.27	0.89	0.78	0.57	0.57	0.35	0.53	0.50	4.38	1.20
		12	200	0.38	137	0.18	0.39	0.18	0.25	0.14	0.18	0.11	0.14	0.11	0.85	0.28
		12	430	0.80	595	0.50	1.06	0.42	0.64	0.39	0.39	0.25	0.42	0.35	2.97	0.85
		15	410	0.80	532	0.35	0.85	0.35	0.46	0.25	0.25	---	---	---	---	---
		15	450	0.87	636	---	---	---	---	---	---	0.28	0.42	0.39	2.83	0.85
		30	190	0.52	117	0.25	0.28	0.42	0.18	0.11	0.18	0.03	0.07	0.07	0.28	0.14
		30	300	0.80	281	0.18	0.42	0.18	0.35	0.21	0.18	0.07	0.14	---	0.85	0.28
	1	30	340	0.89	352	0.21	0.53	0.25	0.29	0.25	0.18	0.11	0.21	0.18	1.27	0.35
	2	0	0	0	0	0.11	0.11	0.11	---	---	---	---	---	---	---	---
		2	195	0.31	129	0.11	0.21	0.18	0.14	0.11	0.18	0.07	0.07	0.07	0.28	0.14
		2	350	0.55	416	0.25	0.57	0.25	0.32	0.18	0.18	0.11	0.18	0.18	1.13	0.28
		2	495	0.78	831	0.53	1.27	0.64	0.74	0.42	0.46	0.28	0.50	0.46	3.68	0.99
		8	440	0.76	636	0.46	0.96	0.42	0.57	0.35	0.28	0.18	0.35	0.32	2.12	0.57
		15	440	0.86	610	0.39	0.78	0.39	0.53	0.32	0.25	0.25	0.35	0.35	3.54	0.78
		29	195	0.52	125	0.11	0.21	0.18	0.14	0.11	0.11	0.07	0.07	0.11	0.57	0.11
		29	300	0.78	279	0.18	0.42	0.18	0.35	0.21	0.18	0.07	0.14	0.18	0.85	0.11
A-7C	2	29	340	0.88	354	0.21	0.57	0.21	0.42	0.25	0.18	0.11	0.21	0.18	1.41	0.18

Table 9. Summary of RMS Fluctuating Pressure Levels on HARPOON Exterior Surface During Captive Flight on Various Aircraft

Aircraft	Wpn Sta.	Flight Conditions: Altitude (kft)	Airspeed (kts)	Mach No.	Dyn. Press. (psf)	RMS Pressure, dB: Guidance Section VA14	VA15	Boattail VA16
P-3C	10	1	140	0.22	66	126	120	126
		1	275	0.42	257	126	126	143
		1	355	0.55	427	134	132	150
		3	350	0.55	416	132	130	149
		15	305	0.61	305	132	132	146
		25	140	0.35	66	126	126	130
	10	25	255	0.62	210	126	130	140
	14	1	140	0.22	66	126	130	130
		1	275	0.42	257	134	132	138
		1	380	0.59	490	141	139	143
		3	210	0.34	150	126	126	130
		3	340	0.54	392	142	141	143
		15	305	0.61	305	138	136	140
		25	140	0.35	140	126	130	126
P-3C	14	25	255	0.62	210	134	134	---
S-3A	5	0	0	0	0	147	126	132
		1	140	0.22	66	126	126	126
		1	275	0.42	257	126	126	138
		1	340	0.52	392	126	130	145

Aircraft	Wpn Sta.	Flight Conditions: Altitude (kft)	Airspeed (kts)	Mach No.	Dyn. Press. (psf)	RMS Pressure, dB: Guidance Section VA14	VA15	VA16
S-3A	5	3	340	0.54	392	126	130	145
		15	314	0.62	326	126	126	141
		25	260	0.63	219	126	126	136
A-7C	1	1	180	0.28	110	126	129	126
		1	350	0.54	416	132	132	138
		1	550	0.85	1026	143	143	154
		12	430	0.80	595	134	129	148
		15	450	0.87	636	134	132	145
		30	190	0.52	117	126	126	134
		30	300	0.80	281	120	120	134
	1	30	340	0.89	352	126	126	137
	2	2	195	0.31	129	126	126	137
		2	350	0.55	416	126	126	140
		2	495	0.78	831	138	132	---
		8	440	0.76	636	130	126	146
		15	440	0.86	610	130	126	146
		29	195	0.52	125	120	120	134
		29	300	0.78	279	120	120	134
	2	29	340	0.88	354	126	126	138

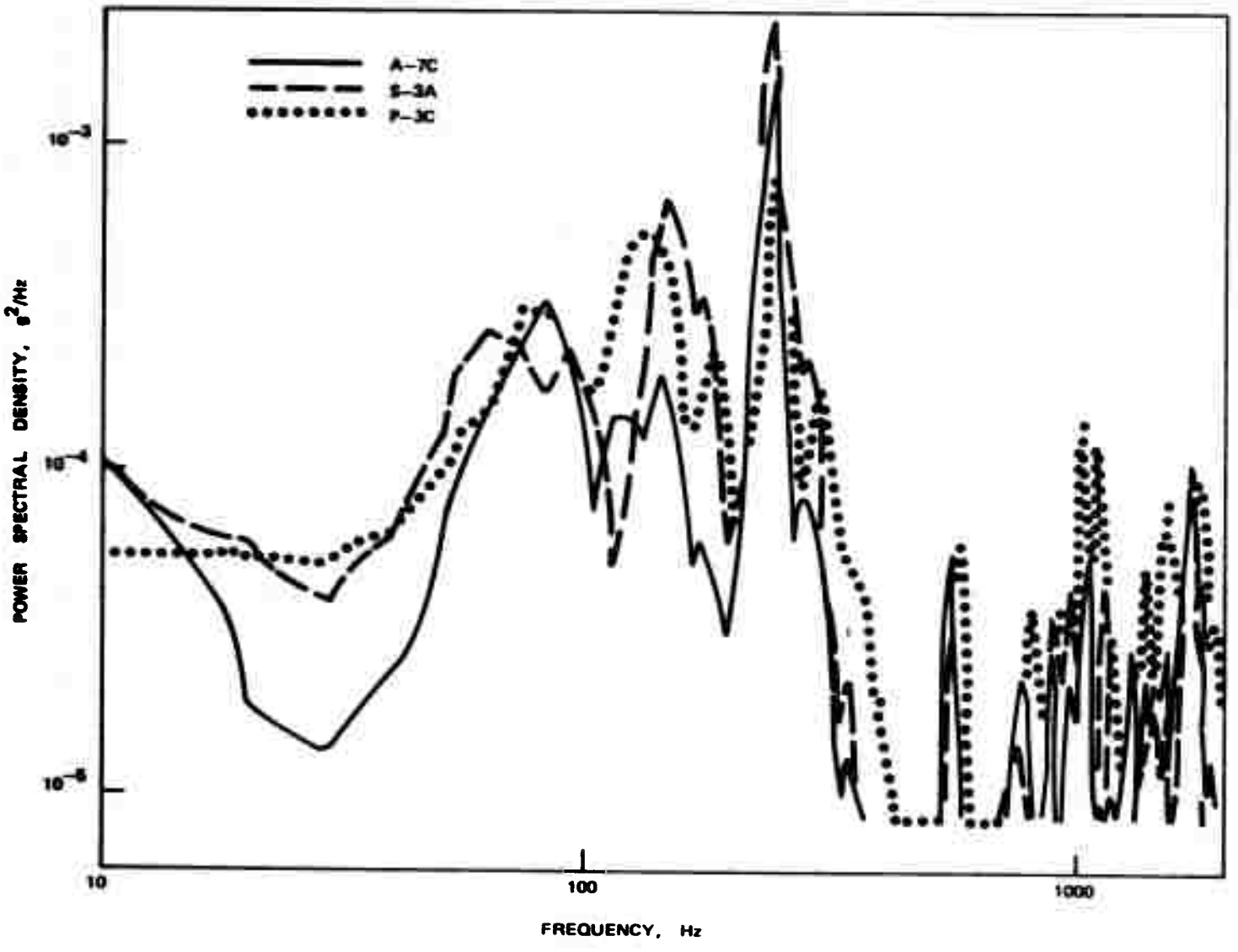

FIGURE 9. Power Spectra of HARPOON Vertical Response at the Seeker Location During Captive Flight on Three Different Aircraft at a Dynamic Pressure of 400 PSF.

measured at the Seeker (VV 35) during captive flight under similar conditions on the three carriage aircraft. Note that the spectra have been standardized to a common dynamic pressure of q = 400 psf using the relationship, $G(f) \approx q^2$ where G(f) is the spectral density at frequency f.

The results in Figure 9 strongly suggest that the carriage aircraft does not have a major influence on the captive flight vibration environment of the missile, at least at the higher frequencies, even though one of the carriage aircraft is propeller driven and the other two are jets. This is consistent with prior studies [7,8] that indicate the vibration environments of external stores carried at relatively high speeds are dominated by aerodynamic forces related primarily to flight dynamic pressure, rather than aircraft propulsion sources. At the lower frequencies, the vibration power spectra for the propeller driven P-3C flights do reveal strong contributions at the P-3C blade passage frequency and its harmonies, at least at some locations, as will be detailed later.

The power spectra of the surface pressure data generally reveal a stronger distinction between the propeller and jet powered carriage aircraft, as demonstrated by the data in Figure 10. This figure presents the power spectra of the pressures measured

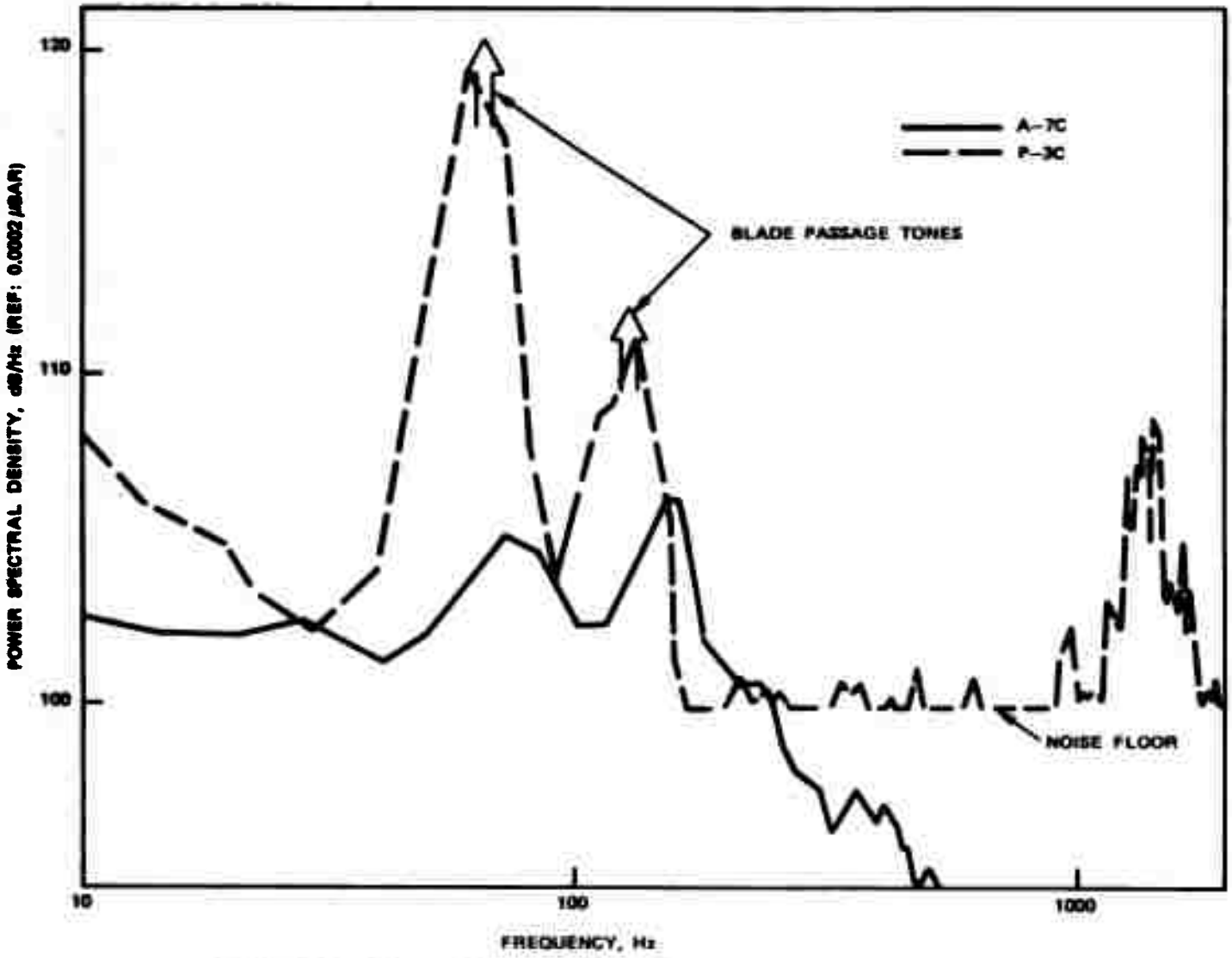

FIGURE 10. Power Spectra of Surface Pressure on HARPOON Guidance Section During Captive Flight on Two Different Aircraft at a Dynamic Pressure of 400 PSF.

on the side of the HARPOON guidance section during captive flight on the jet powered A-7C and the propeller driven P-3C aircraft. Again, the data have been standardized to a common flight dynamic pressure of q = 400 psf. Note that the pressure spectrum for the P-3C flight test is dominated by tones at about 65 and 130 Hz, corresponding to the P-3C propeller blade passage frequency and its first harmonic. On the other hand, the pressure spectrum for the A-7C flight test is smoother with characteristics similar to separated boundary layer turbulence [7]. There are small peaks in the spectrum at about 75 and 150 Hz which probably represent tonal contributions related to the jet engine shaft rotation.

5.4 Gunfire Tests

The rms vibration levels measured at the six accelerometer locations in the seeker and guidance section, and the rms pressure levels measured by the three pressure transducers during captive flight on the A-7C aircraft with and without gunfire are summarized in Table 10. It is seen from this table that a gunfire burst with a rate of 4000 rounds/min. caused the rms vibration levels on the seeker bulkhead to increase by over 100% on the average. For a firing rate of 6000 rounds/min., the rms vibration levels in the guidance section and the rms pressure levels at the three pressure

Table 10. Summary of rms Vibration and Surface Pressure Levels on HARPOON Structure Before and During Gunfire of A-7C Aircraft

Type of Measurement*	Measurement Location		Direction	Gun-fire rate (rpm)	rms acceleration (g) or rms pressure (dB)	
	Description	No.			before gunfire	during gunfire
Vibration	Seeker Bulkhead	VV 33	Axial	4000	0.80 g	1.25 g
		VV 34	Lateral	4000	1.50 g	2.80 g
		VV 35	Vertical	4000	0.60 g	2.15 g
	MGU Mounting Structure	VV 36	Axial	6000	0.80 g	1.10 g
		VV 37	Lateral	6000	0.55 g	1.35 g
		VV 38	Vertical	6000	0.60 g	0.80 g
Fluctuating Surface Pressure	Guidance Section	VA 14	Top	6000	145 dB	149 dB
		VA 15	Side	6000	139 dB	145 dB
	Boattail	VA 16	Side	6000	150 dB	153 dB

*All measurements made during straight and level flight at 1000 ft. with a dynamic pressure of 700 psf.

transducer locations were increased by about 70% on the average. It should be noted that these increases were recorded during captive flight at a dynamic pressure of q = 700 psf, which produced relatively high vibration levels even without gunfire.

The power spectra of the vibration and pressure measurements before and during gunfire indicate that the gunfire increases the vibration levels over a wide frequency range, although the greatest increase does occur at the gun firing rate frequency. This is illustrated in Figure 11, which shows the power spectrum of the vibration measured before and during gunfire at 4000 rounds/min. at the location showing the greatest increase due to gunfire, namely, the vertical measurement on the seeker bulkhead (VV 35). In this figure it is seen that the gunfire levels are higher at most frequencies, but particularly at 67 Hz., the frequency of the gun firing rate.

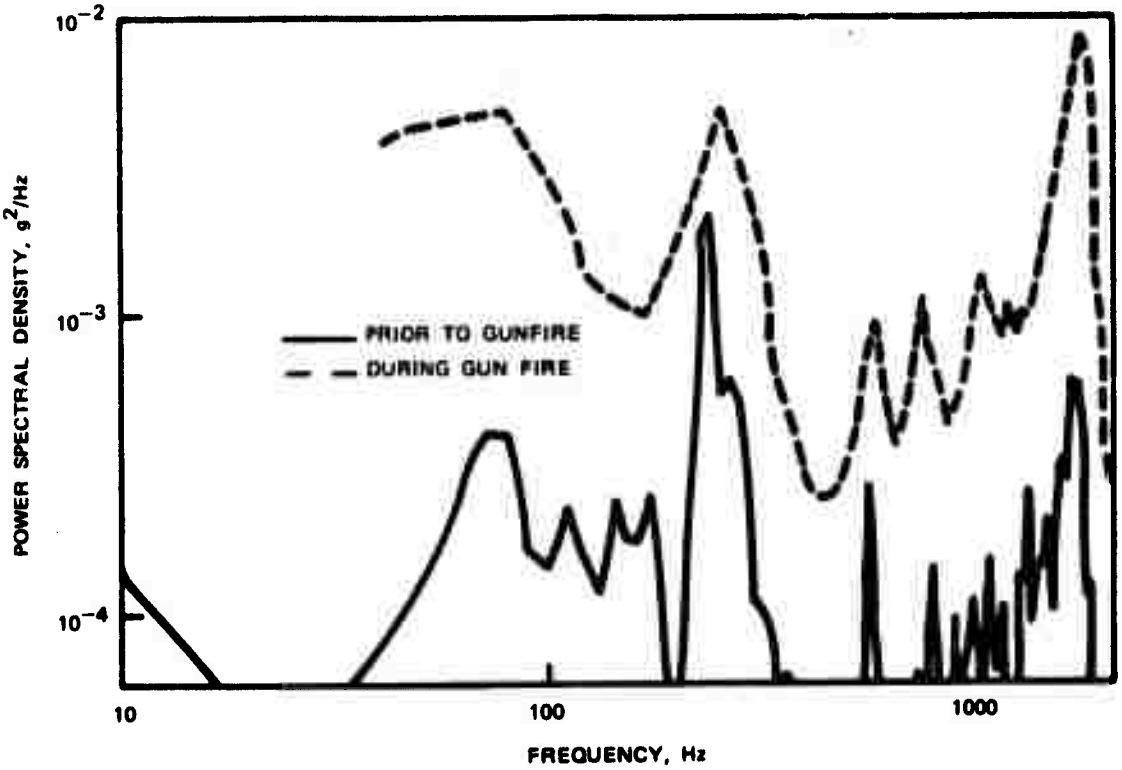

FIGURE 11. Power Spectra of HARPOON Vertical Response at the SEEKER Location During Captive Flight on A-7C at a Dynamic Pressure of 700 PSF.

6. EVALUATION OF RESULTS

Of primary interest in the test results are possible correlations of the measured missile response levels (shock, vibration and/or fluctuating pressure levels) with pertinent test conditions, such as (a) the carriage aircraft used for the tests, (b) the missile location on the aircraft, (c) the flight condition of the aircraft, and (d) the measurement location on the missile. These various correlations were investigated for the catapult launch and arrested landing tests using peak acceleration levels and shock spectra, and for the captive flight and gunfire tests using rms levels and power spectra.

For those evaluations involving shock or power spectra, averages were performed using the logarithms of the spectral levels rather than their absolute values. This was done because past studies [1,7,8] indicate that the spatial distribution of narrow band shock and vibration levels over an airborne missile structure tends to be lognormal in character; i.e., the logarithms of the spectral levels tend to be normally distributed. In other cases where overall rms values were involved, and the variance of the data to be averaged was relatively small, the averages were computed using mean

square values, that is, average rms = $[rms_1^2 + rms_2^2 + \ldots]^{1/2}$.

Finally, to permit the evaluations to be performed in an efficient manner, all vibration and surface pressure spectral data were reduced to maximum spectral density values in one-third octave bands, and then keypunched for statistical analysis on a digital computer. All such statistical evaluations were performed using the well known UCLA BMD statistical data analysis programs.

6.1 Catapult Launch Data

Referring to Table 3, all catapult launch tests were performed using a single aircraft and missile mounting location. Furthermore, since there were only slight variations in the maximum launch acceleration, aircraft speed, and aircraft gross weight among the four tests detailed in Table 3, the missile response was not measured at any given location for more than one set of launch conditions. Hence, the data are not adequate to evaluate possible relationships between the missile response and the aircraft configuration or launch conditions. On the other hand, since the variation in the launch conditions from test to test was slight, the data do provide a basis for assessing the variations in the missile response environment

as a function of location on the missile structure. This is done in Figure 12 using the peak acceleration data taken from Table 6.

It is seen from Figure 12 that the peak acceleration response of the missile in the vertical and lateral directions is most intense at the forward end of the missile. From the time history data in Figure 4, the dominant frequency of the response is about 10 Hz. These data suggest that the missile is responding to the catapult launch primarily at a fundamental normal mode of the missile-rack-aircraft combination, which results in both pitching and yawing of the missile, or perhaps missile bending. On the other hand, the peak acceleration levels in the axial direction are relatively uniform in level over at least the first 70 inches of the missile. This would be expected since the missile, rack, and aircraft wing are very stiff in the axial direction. Note that the average peak acceleration in the axial direction (about 4 to 5 g) is slightly less than the peak longitudinal acceleration of the aircraft (about 5 to 6 g). This discrepancy is probably due to the fact that the aircraft acceleration axis during a catapult launch does not lie along the missile axis.

Now considering the data in terms of shock response levels, the

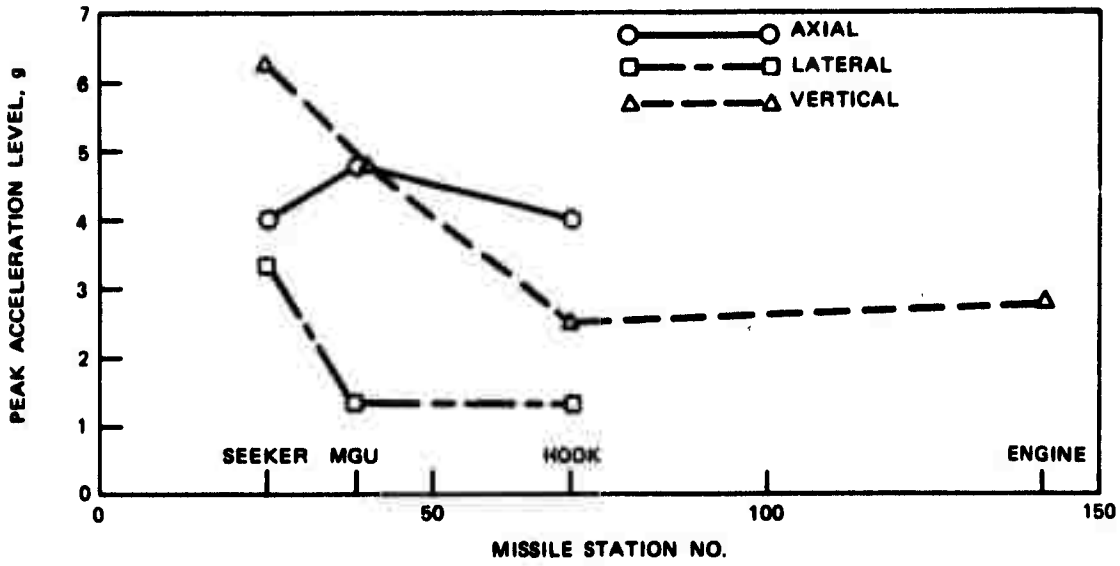

FIGURE 12. Peak Missile Response Level Versus Location on HARPOON Missile During Catapult Launches of A-7E Aircraft.

Q = 10 shock spectra of the missile response at the seeker, MGU, and forward hook locations are shown for each of the three orthogonal axes in Figure 13. Note that the levels in the vertical direction are generally higher than the lateral and axial levels at the lowest frequencies, but the levels at the higher frequencies are similar along all three axes. Furthermore, the levels at the three different locations are not as different as might have been expected from the peak acceleration data in Figure 12.

There is only a small amount of prior data available on the shock response of airborne missiles during catapult launches of their carriage aircraft which can be considered reliable. Limited measurements of the shock response of a Standard ARM missile on an A-6 aircraft indicate higher levels than those shown in Figure 13. There is a general design criterion for catapult launch loads on wing mounted missiles provided by MIL-A-8591D [9]. The design criterion are stated in terms of design limit load factors which are shown with the shock response spectra for the forward hook location in Figure 13. Note that the shock spectra values in all three directions generally fall within the design criterion at most frequencies below 500 Hz.

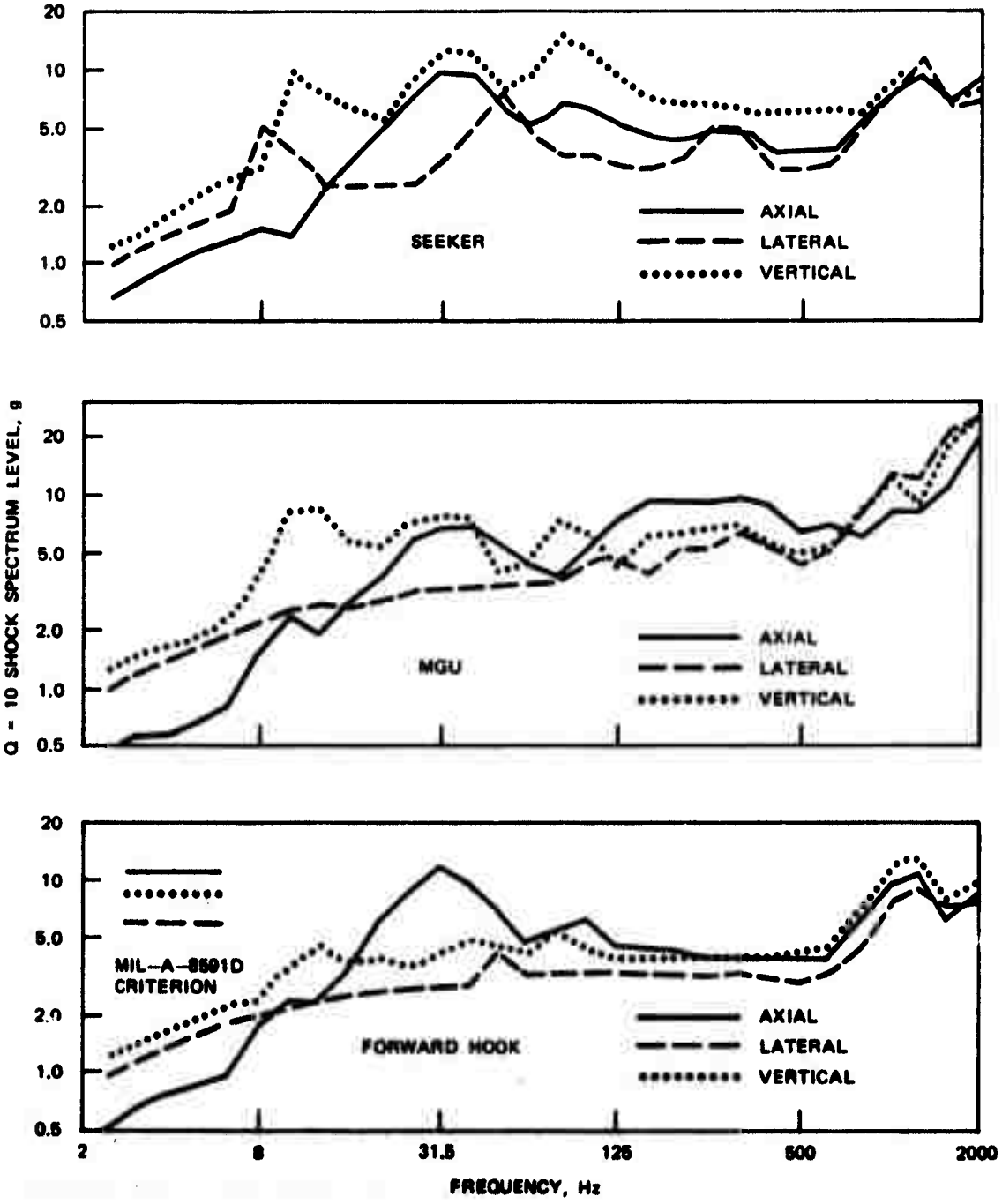

FIGURE 13. Q=10 Shock Spectra of the HARPOON Missile Response During Catapult Launches of an A-7E Aircraft.

6.2 Arrested Landing Data

Referring to Table 4, all arrested landings were performed using a single aircraft and missile mounting location, and there were only slight variations in the maximum deceleration and aircraft gross weight among the ten tests. However, referring to Table 7, repeated measurements were made at a single location (the forward hook) for five different landings, including one landing with a very low sink rate (2.4 ft./sec.). Hence, the data can be evaluated for a dependence on aircraft sink rate as well as the measurement location on the missile.

First concerning a dependence on aircraft sink rate, visual inspection of the data in Table 7 measured at the forward hook location does not reveal a significant dependence of the missile response acceleration on sink rate, at least in the axial and lateral directions. In the vertical direction, the one acceleration measurement for the sink rate of 2.4 ft/sec is about half the measurements at higher sink rates. However, a correlation analysis of all the peak acceleration versus sink rate data at the hook location does not reveal a statistically significant correlation at the 5% level of significance. Hence, it must be concluded that the dependence, if any, of the missile response on the aircraft sink rate is

too weak to be revealed by the available data.

Now concerning possible variations in the missile response levels with measurement location, the average of the peak acceleration levels along the three axis at each measurement location are shown in Figure 14. These results were obtained by averaging together the data in Table 7 for different landing sink rates, excluding the data for the sink rate of 2.4 ft/sec. It is seen from Figure 14 that the missile response during arrested landings is similar in spatial distribution to the response levels measured during catapult launches, as shown earlier in Figure 12; specifically, the maximum response levels occur at the seeker with the lateral levels being somewhat lower than the axial and vertical levels. In this case, however, the peak acceleration levels in the axial direction are about the same as the maximum aircraft deceleration levels measured during the arrested landings.

The Q = 10 shock spectra of the missile response at the seeker, MGU, and forward hook locations are shown for each of the three orthogonal axes in Figure 15. The spectra are for those tests which produced at highest peak acceleration levels measured at each location. As for the catapult launch results, the shock spectra shown in Figure 15 do not vary

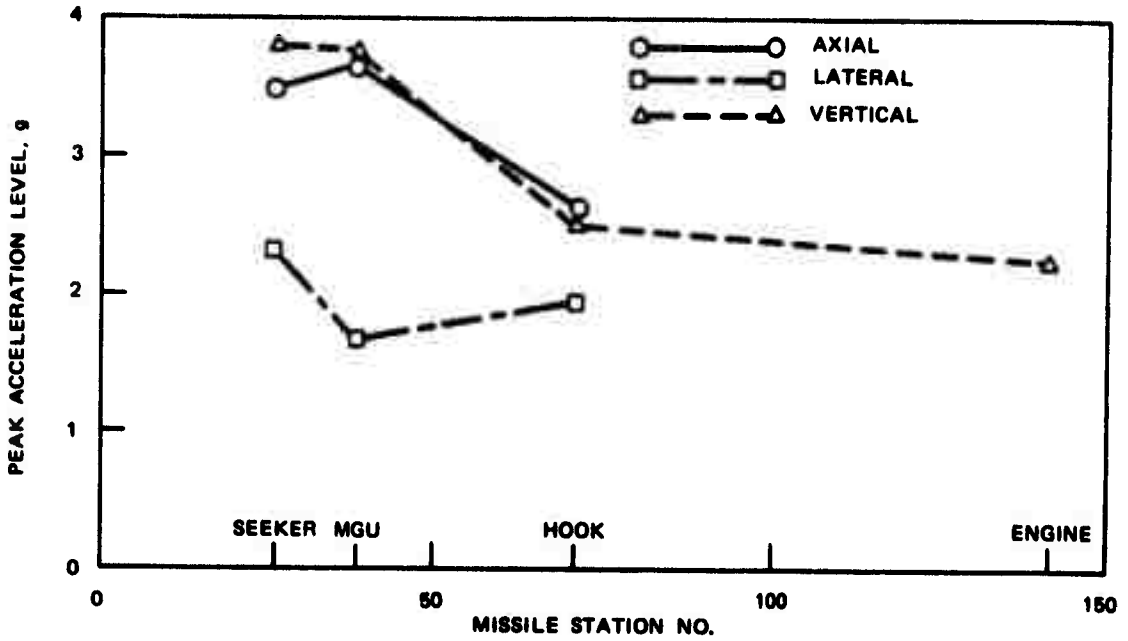

FIGURE 14. Peak Missile Response Level Versus Location on HARPOON Missile During Arrested Landings of A-7E Aircraft.

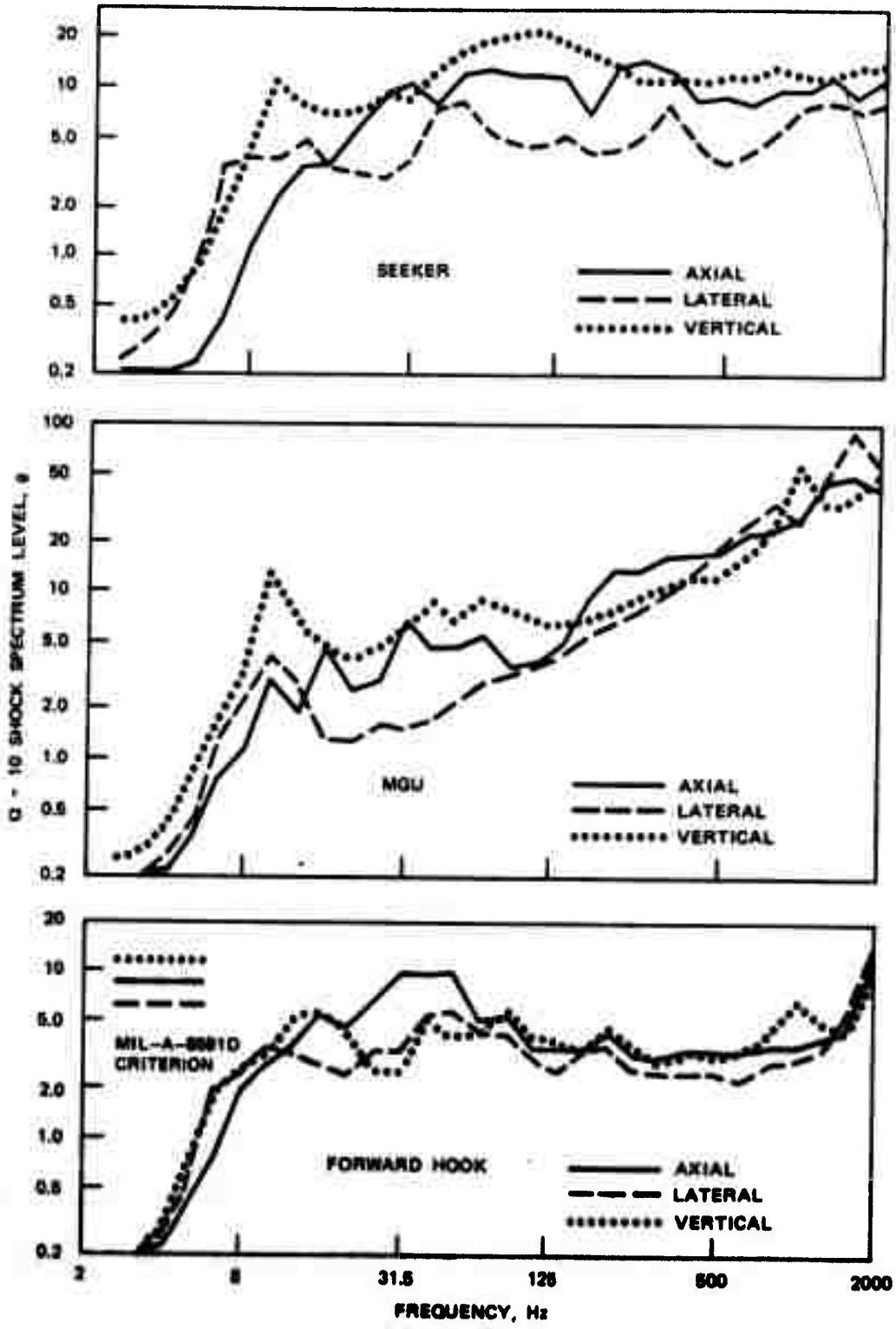

FIGURE 15. Q=10 Shock Spectra of HARPOON Missile Response During Arrested Landings of A-7E Aircraft.

dramatically from one location to another at a given frequency.

The MIL-A-8591D design limit load factors for arrested landing loads on wing mounted missiles are shown with the shock response spectra for the forward hook location in Figure 15. Note that the design criterion exceeds the shock spectra levels in all directions and at almost all frequencies. Furthermore, the arrested landing criterion exceeds, at most frequencies, the measured shock spectra levels during catapult launches as well. Hence, it can be said that both the catapult launch and arrested landing loads are within the general design criteria of MIL-A-8591D.

6.3 Captive Flight Vibration Data

Referring to Table 8, considerable captive flight vibration data were collected for three different aircraft operating under a wide range of flight conditions, including take-off. For the A-7C aircraft, the vibration levels during take-off are substantially lower than the flight vibration levels at all frequencies and, hence, can be ignored. For the P-3C aircraft, the take-off vibration levels are lower than the flight levels at all frequencies above 30 Hz. At frequencies below 30 Hz, the take-off levels sometimes exceed the levels

during straight and level flight by a factor of two, but are still lower than the flight levels during a turn. Hence, the take-off vibration can be ignored for the P-3C as well. No take-off vibration data are available for the S-3A aircraft.

For straight and level flight, the vibration data for all three aircraft collapse quite well as a function of dynamic pressure. This is illustrated using overal rms values averaged over all eleven accelerometer locations in Figure 16. The dashed line on each plot in this figure represents the least squares regression line for vibration level (g rms) versus dynamic pressure (q) with an intercept of zero.

There are several aspects of the data in Figure 16 which should be noted. First, there is no significant difference in the measured vibration levels versus dynamic pressure for captive flight on two different weapons stations of the same aircraft. Second, the measured vibration levels versus dynamic pressure are about the same for captive flight on the A-7C and S-3A aircraft. Third, the measured vibration levels for captive flight on the propeller driven P-3C aircraft display a strong dependence on dynamic pressure, although the slope of the dependence is slightly greater than occurs for the two jet powered aircraft. These results confirm the conclusions drawn from data for other missiles [7,8]

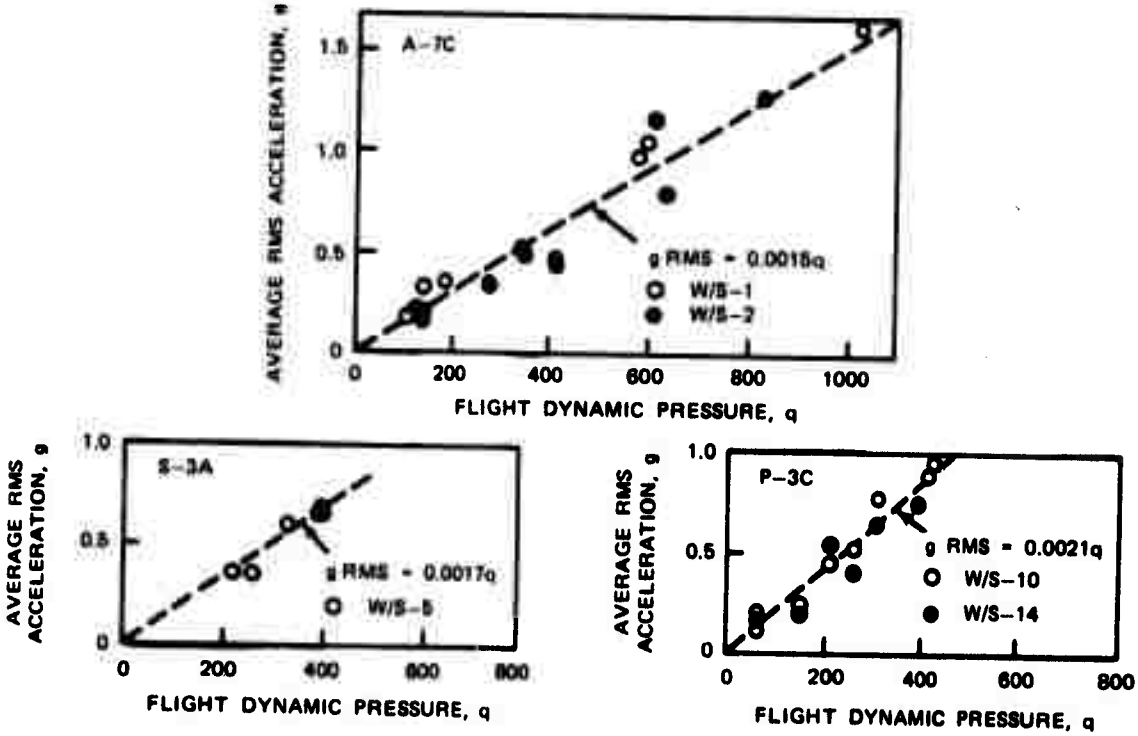

FIGURE 16. RMS Vibration Levels Versus Dynamic Pressure For the HARPOON Missile During Captive Flight on Three Different Aircraft.

that the captive flight vibration environment of externally carried stores is due primarily to aerodynamic excitation and, hence, is relatively independent of the carriage aircraft and mounting location. This appears to be true even for captive flight on a propeller driven aircraft such as the P-3C, at least in terms of the overall vibration levels.

When considered in terms of frequency spectra, some differences do appear in the HARPOON captive flight vibration environment among the three carriage aircraft at the lower frequencies. This is illustrated in Figure 17, which presents the power spectrum averaged over all eleven measurement locations for the vibration during captive flight on each of the three aircraft operating at a common flight dynamic pressure of $q = 400$ psf. Note that the average power spectra of the vibration environments are remarkably similar (within $\pm$ 1 dB) at all frequencies above 200 Hz. Below 200 Hz, however, there are some significant differences. Specifically, the spectral levels of the captive flight vibration during carriage on the propeller driven P-3C aircraft are substantially higher than for the two jet powered aircraft, reflecting the added contribution of propeller noise excitation to the HARPOON vibration levels. Indeed, the first and second propeller blade passage frequencies are clearly apparent in

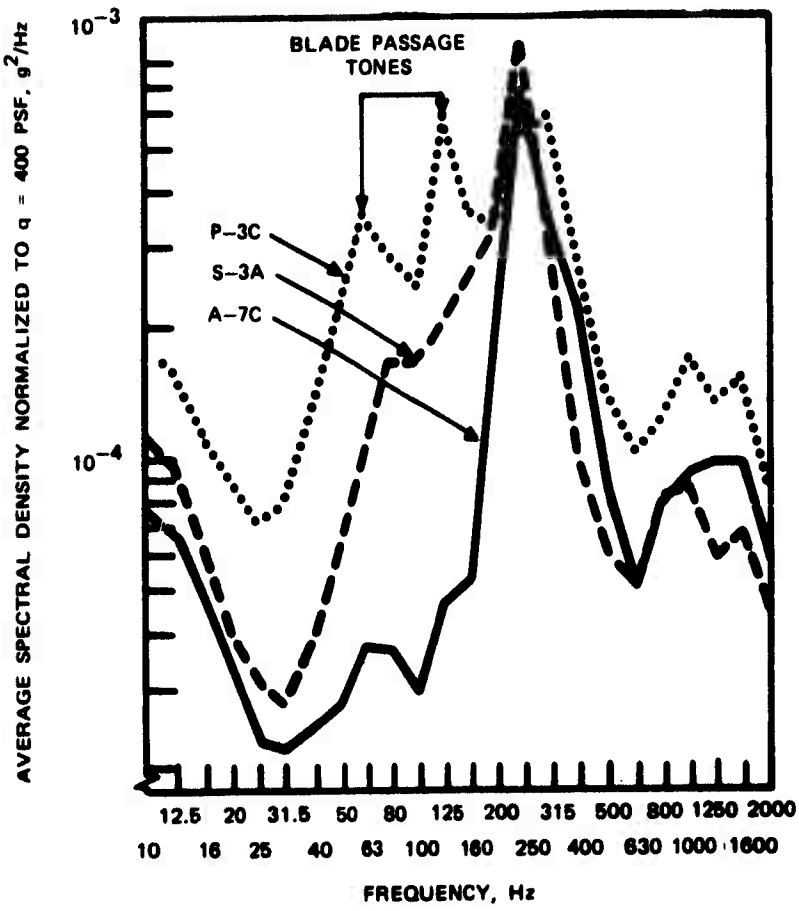

FIGURE 17. Average Power Spectra of HARPOON Missile Vibration During Captive Flight On Three Different Aircraft.

the P-3C vibration data. There is also a significant difference between the average spectral levels during carriage on the S-3A and A-7C jet aircraft in the frequency range between 50 and 200 Hz, with the S-3A levels being higher. This undoubtedly reflects the added contribution of engine noise during the S-3A carriage; i.e., the missile is carried at a location adjacent to the wing mounted engine on the S-3A aircraft, as illustrated in Figure 3.

The results presented in Figure 17 are for straight and level flight. The vibration levels during a sharp turn of the aircraft are substantially greater in the frequency range below 200 Hz due to the low frequency buffet induced by a turn maneuver. This is demonstrated in Figure 18 which shows the average power spectra of the vibration measured on the seeker bulkhead during level flight and a 5.5 g turn of the A-7C aircraft. Note that the spectral data in this figure have been standardized to a common dynamic pressure of q = 716 psf, which was the actual dynamic pressure during the 5.5 g turn. It is clear from these results that the low frequency vibration of the HARPOON missile is strongly amplified by buffet producing maneuvers.

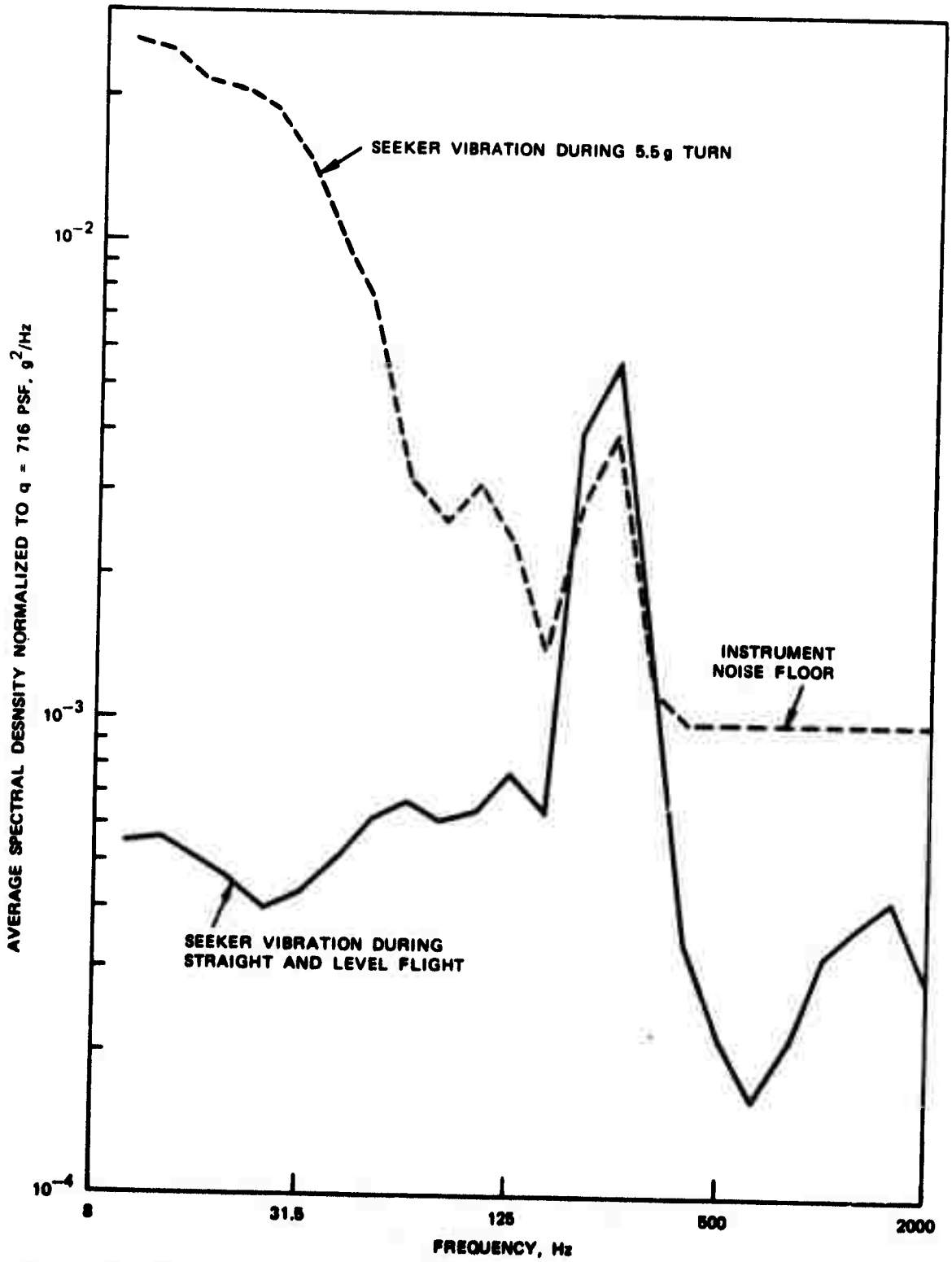

FIGURE 18. Average Power Spectra of HARPOON Missile Vibration at Seeker During Captive Flight on A-7C Aircraft in Turn.

Now consider the spatial variations of the vibration data over the length of the HARPOON structure. These spatial variations are shown in terms of overall vibration levels in Figure 19, where the data for the two jet powered aircraft are pooled together because of their similarity. The data in Figure 19 indicate that the vibration levels along the three orthogonal axes are relatively homogeneous in the forward half of the missile during captive flight on all three aircraft. The only exception is the lateral measurement on the seeker bulkhead which tends to be about twice as high as the other measurements in the forward region. In the aft region of the missile, however, the only available radial direction measurement (VV 40 on the motor) is about four times greater than the general vibration levels in the forward region. These data are consistent with the results of past studies [7] that indicate the captive flight vibration environment of missile is significantly more intense in the aft end of the missile than in the forward and mid regions.

The spatial variations of the missile vibration from one location to another are further investigated in terms of their power spectra in Figure 20. In this figure, the power spectra of the vibration measured along the three orthogonal axes are pooled together to arrive at a single average spectrum at the seeker, MGU, and forward hook locations for each of

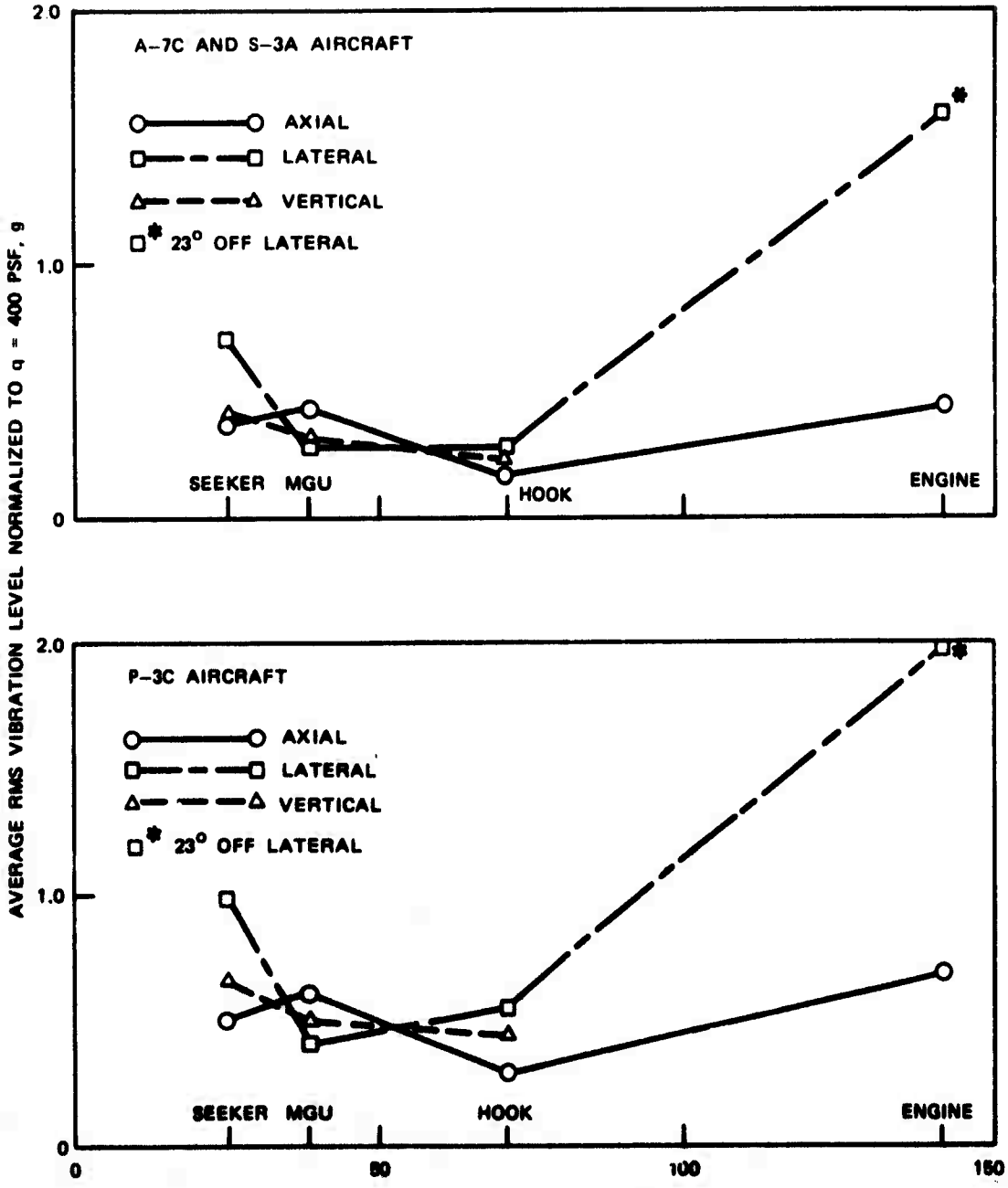

FIGURE 19. Average RMS Vibration Levels Versus Location on HARPOON Missile During Captive Flight on Three Different Aircraft.

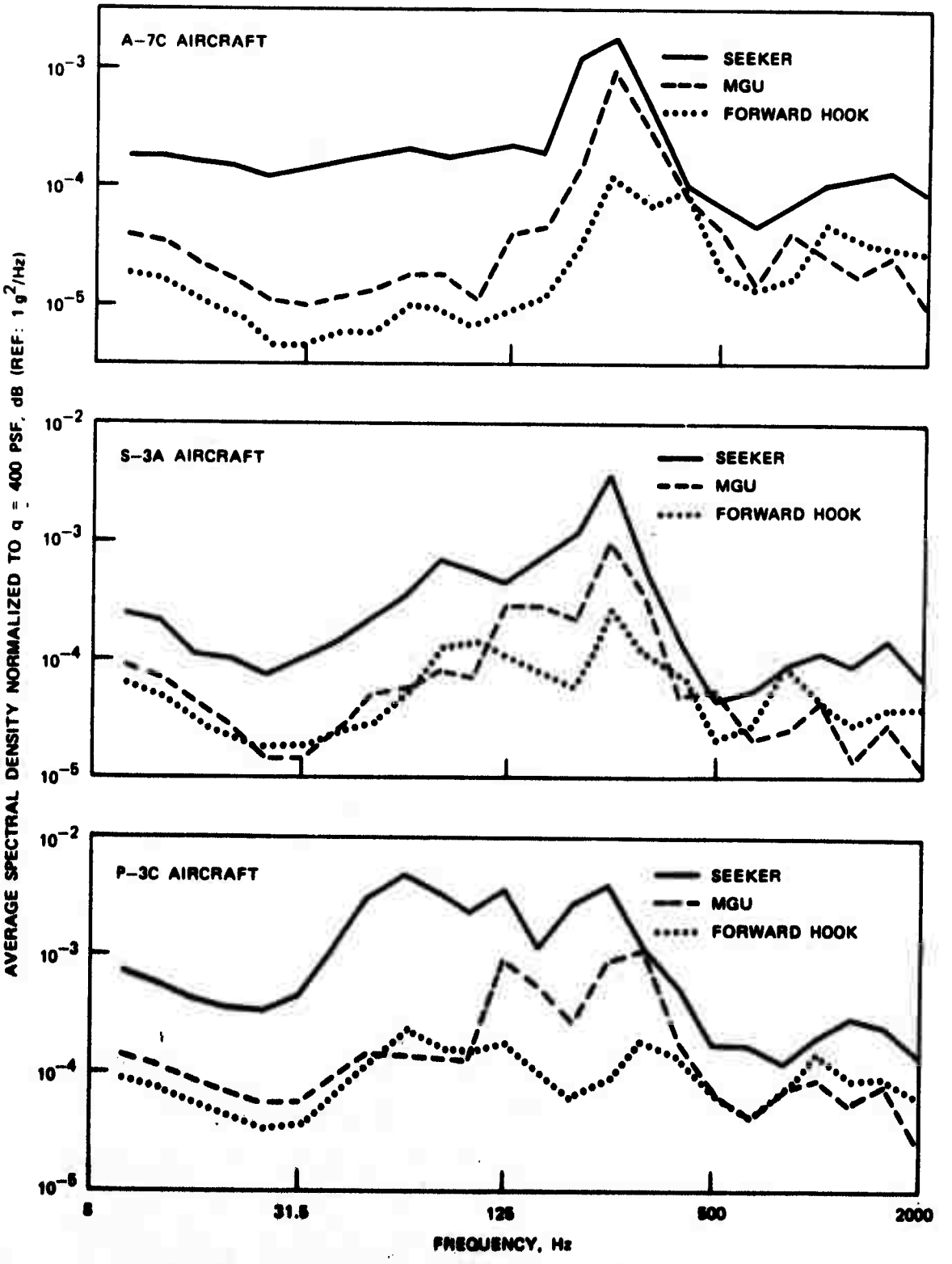

FIGURE 20. Average Power Spectra of Vibration Levels at Various Locations on HARPOON Missile During Captive Flight on Three Different Aircraft.

the three carriage aircraft operating at a common flight dynamic pressure of q = 400 psf. Note that the vibration levels at the higher frequencies (above about 400 Hz) are similar in magnitude from one location to another for a given carriage aircraft. At the lower frequencies, however, the seeker vibration levels are higher than those at the MGU and forward hook by about 10 dB.

A final point of interest is a comparison of the HARPOON captive flight vibration levels with data for other externally carried aircraft stores, as well as with the test requirements of the proposed MIL-STD-810C [10]. To make these comparisons, the vibration levels measured at the seeker, MGU, and forward hook locations during captive flight on the two jet aircraft (A-7C and S-3A) were pooled together after scaling the data to a common flight dynamic pressure of q = 1200 psf. The maximum spectral density level in each of 24 contiguous one-third octave band intervals was then determined from the pooled data. These results are compared to the 95% tolerance level determined for pooled data from 12 other externally carried aircraft stores [7] in Figure 21. Also shown in Figure 21 is the test requirement specified for captive flight vibration environments of externally carried stores by MIL-STD-810C [10]. In all cases,

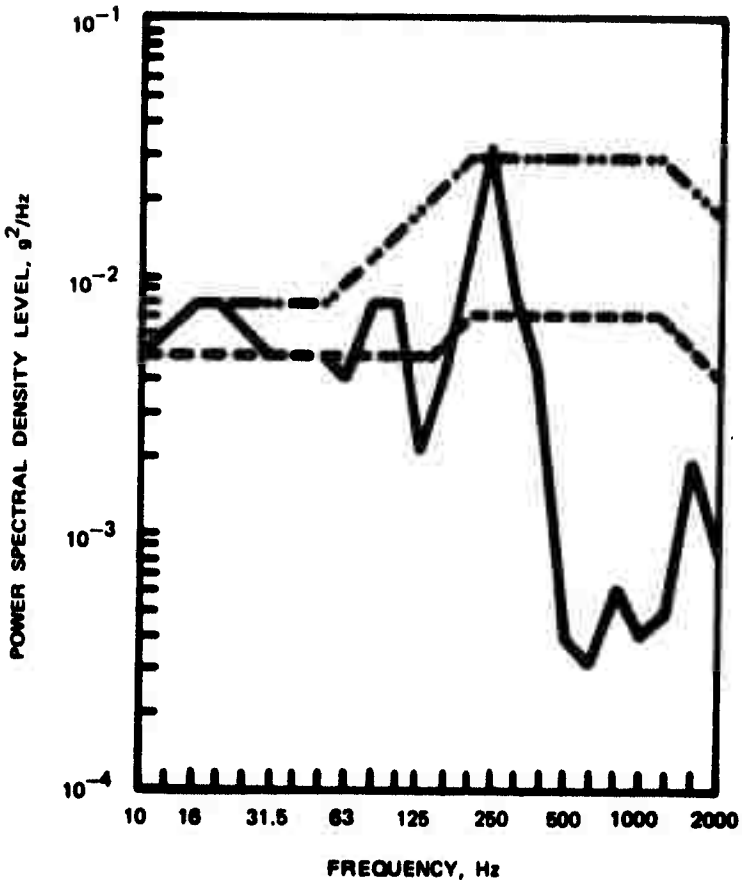

FIGURE 21. Comparison of Maximum Power Spectra for HARPOON Captive Flight Vibration with Data For Other Missiles and MIL-STD-810C Test Levels.

the comparisons are based upon an average missile weight density of w = 100 pcf and a flight dynamic pressure of q = 1200 psf. These values constitute the approximate weight density of the HARPOON missile, and the approximate maximum dynamic pressure for captive flight on an A-7C aircraft.

The results in Figure 21 indicate that the maximum spectral density levels of the HARPOON captive flight vibration environment generally exceed the test requirements of MIL-STD-810C at frequencies below 400 Hz. However, the HARPOON levels at these lower frequencies are bounded with reasonable accuracy by the smoothed envelope determined from prior data for other airborne missiles. On the other hand, at frequencies above 400 Hz, the maximum spectral density levels of the HARPOON vibration fall far below both the envelope for other data and the MIL-STD-810C test requirements. The reason for this lack of high frequency response of the HARPOON missile may be related to the fact that it is larger than most of the prior missiles used to generate the data pool for Ref. 7 and MIL-STD-810C.

6.4 Captive Flight Surface Pressure Data

Referring to Table 9, fluctuating surface pressures were measured at three locations on the HARPOON missile during

captive flight under various conditions on the three carriage aircraft. These pressure measurements are shown as a function of flight dynamic pressure in Figure 22. Note that the two measurements on the surface of the guidance section have been averaged because they are generally similar. Further note that an approximate regression line constrained to the theoretically expected slope of 6 dB per doubling of dynamic pressure is superimposed on each plot.

The data in Figure 22 reveal a dependence on dynamic pressure, although the correlation is not as strong as was previously indicated for the rms vibration levels shown in Figure 16. The greater scatter in the fluctuating pressure data is to be expected since point pressure measurements are sensitive to local perturbations in the aerodynamic excitation, while structural vibration measurements tend to reflect a response to the average excitation distributed over the structure. Nevertheless, the results are generally consistent with past data for externally carried aircraft stores [7], as well as the acoustic test requirements of the proposed MIL-STD-810C [10]. Comparisons with these past data and MIL-STD-810C, Method 515.2, are presented in Table 11.

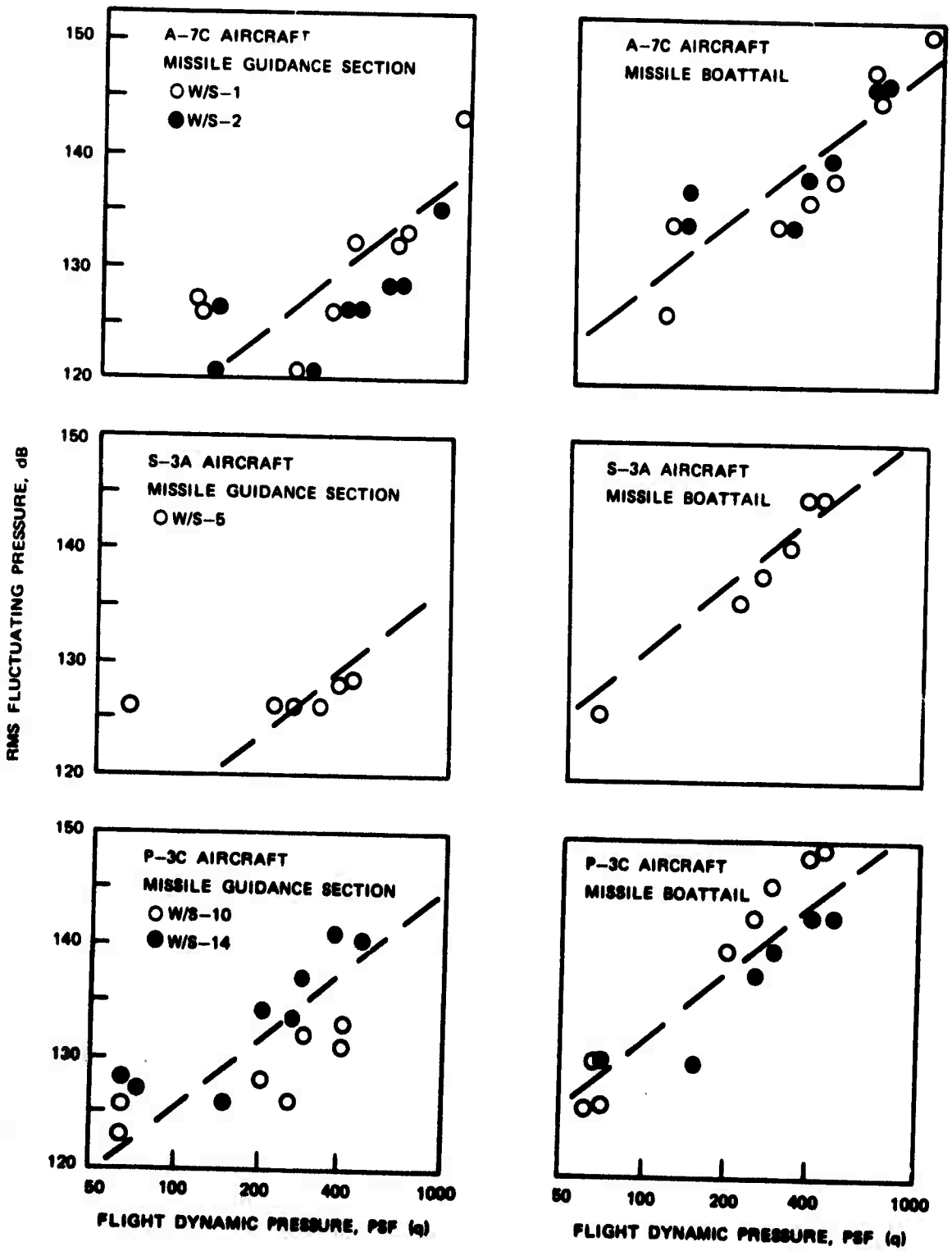

FIGURE 22. RMS Pressure Levels Versus Dynamic Pressure For the HARPOON Missile During Captive Flight on Three Different Aircraft.

Table 11. Comparison of HARPOON Captive Flight Surface Pressure Levels With Past Data and MIL-STD-810C Test Requirements

Aircraft	Location	Measured HARPOON Overall Pressure Levels Normalized To q = 400 psf (95% Confidence Interval, dB)	Max OA Level From Ref. 7 for q = 400 psf (dB)	MID STD 810C Requirement for q = 400 psf* (dB)
A-7C	Guid. Section	127.4 to 131.0	142	146
	Boattail	139.3 to 142.9	142	146
S-3A	Guid. Section	127.6 to 130.4	142	146
	Boattail	141.2 to 144.8	142	146
P-3C	Guid. Section	135.7 to 138.9	142	146
	Boattail	142.5 to 147.1	142	146

*Overall level computed using Method 515.2 assuming cylindrical shell with high frequency roll-off starting at 1000 Hz.

From Table 11, it is seen that the fluctuating pressure levels measured on the boattail section are in good agreement with past data and, in some cases, with the test requirements of MIL-STD-810C. On the guidance section, the MID-STD-810C requirements are about 6 dB higher than the measured levels for the two jet powered aircraft. However, the agreement is quite close on the boattail. For the propeller driven P-3C, the agreement is excellent at both locations, when considered only in terms of overall pressure levels. Of course, the spectral levels for the P-3C test exceed the requirements of MIL-STD-810C at the low frequencies because the standard was not designed for captive flight environments on propeller aircraft.

6.5 Gunfire Data

Referring to Table 10, the operation of the A-7C aircraft Gatling gun increased the vibration levels in the forward region (seeker and guidance sections) of the HARPOON missile by about 100% above the normal levels for captive flight at a dynamic pressure of q = 700 psf. There is very little reliable prior data on the gunfire induced vibration environments of airborne missiles available for comparison. Furthermore, the proposed MIL-STD-810C [10] does not address this specific case directly. However, MIL-STD-810C, Method 519.2,

does provide test criteria for the gunfire induced vibration environment for aircraft equipment. Assuming a separation distance between the store and gun nozzle of about 100 inches, MIL-STD-810C yields the test criteria shown in Table 12.

The data in Table 12 display reasonable agreement between the measured gunfire induced vibration of the HARPOON missile and MIL-STD-810C test requirements, depending upon how one chooses to make a necessary weight correction. If the entire HARPOON missile is considered a component, then the MIL-STD-810C requirements would exceed four of the six measurements, but fall short of two measurements by up to 3:1 on the peak spectral density and $\sqrt{3:1}$ on the rms value. However, if the individual sections of the HARPOON missile are considered separate components, then the MIL-STD-810C requirements would be highly conservative at all locations.

Table 12. Comparison of HARPOON Captive Flight Vibration During A-7C Gunfire With MIL-STD-810C Test Requirements

Location	Direction	Measured HARPOON Vibration Levels		MIL STD 810C Requirements**	
		rms level (g)	max. spectral density, (g^2/Hz)	rms level (g)	max. spectral density, (g^2/Hz)
Seeker Bulkhead	axial	1.25	-	1.6 to 6.2	-
	lateral	2.80	0.0071*	1.6 to 6.2	0.0021 to 0.033
	vertical	2.15	-	1.6 to 6.2	
Guidance Section	axial	1.10	-	1.6 to 6.2	-
	lateral	1.35	-	1.6 to 6.2	-
	vertical	0.80	-	1.6 to 6.2	-

*Highest spectral density measured at any of the six loations.

**Requirements of Method 519.2 involve a component weight correction. The lower value assumes the HARPOON is a component. The higher value assumes the seeker and guidance sections are individual components.

7. COMPARISONS TO DESIGN CRITERIA

In the previous section, the measured responses of the HARPOON missile to various environmental loads were evaluated and compared to prior data and the requirements of general design criteria and test specifications for externally carried aircraft stores. Of interest now is a comparison of the maximum anticipated responses of the missile to the applicable design criteria for the HARPOON missile [2].

7.1 Catapult Launch and Arrested Landing Environment

The HARPOON design criteria document [2] specifies that the missile must meet the requirements of MIL-A-8591D for catapult launch and arrested landing loads. A comparison to the requirements of MIL-A-8591D based upon Q = 10 shock spectra for the missile response during catapult launch and arrested landing operations has already been presented in Figures 13 and 15. The measured data are generally consistent with the criteria.

Beyond the MIL-A-8591D requirements, the HARPOON design criteria document [2] specifies carrier handling and storage shock requirements and launch ejection shock requirements which are generally more severe at the lower and higher

frequencies, respectively, than the requirements of MIL-A-8591D. The Q = 10 shock spectra for these two additional requirements are superimposed on the envelope shock spectrum for catapult launch and arrested landing measurements in Figure 23. Excluding a slight violation at 10 Hz, these storage and launch ejection criteria comfortably exceed the measured shock spectra at all locations and frequencies. It is clear from these results that the catapult launch and arrested landing loads are well covered by the HARPOON design criteria taken as a whole.

7.2 Captive Flight Vibration Environment

The HARPOON design criteria document [2] specifies maximum captive flight vibration levels in terms of a power spectrum for the vibration at the forward lug (hook). Hence, the desired comparison here is to the worst case vibration levels which might occur at the forward hook during captive flight, including takeoff, on the three carriage aircraft involved in the experiments. No data are available for the vibration levels at the forward hook location during take-off. However, as discussed in Section 6.3, the vibration levels at other locations where take-off data are available indicate the take-off data are substantially lower than the vibration levels which occur during high dynamic pressure flight.

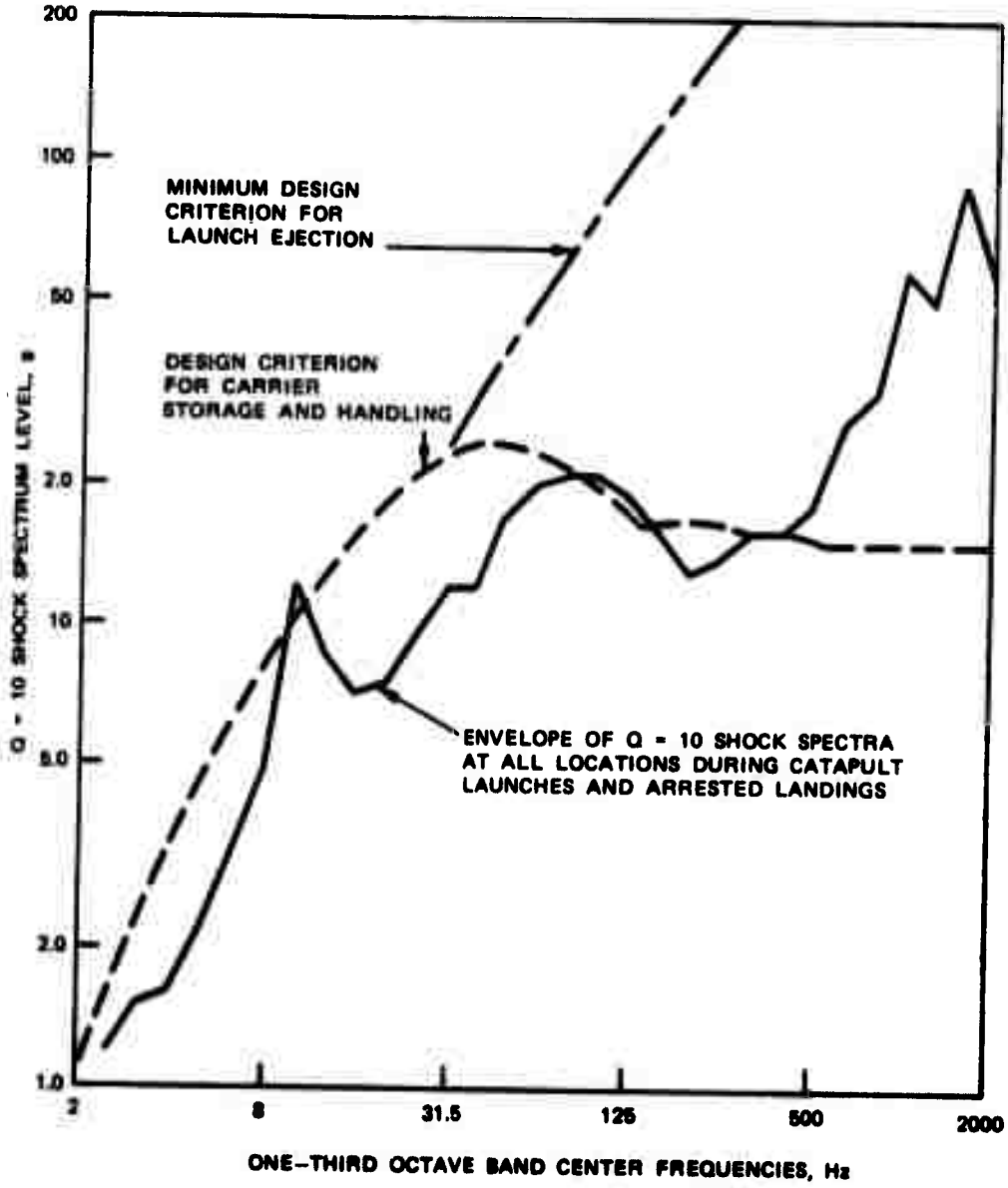

FIGURE 23. Comparison of Catapult Launch and Arrested Landing Shock Loads to HARPOON Environmental Design Criterion.

For the aircraft involved in these experiments, the A-7C is capable of the highest flight dynamic pressure, estimated to be about 1200 psf. The envelope of the maximum spectral density levels of the vibration measured at the forward hook locations for this condition are shown in comparison to the design criteria levels in Figure 24. Note that the A-7C vibration levels at the flight dynamic pressure of q = 1200 psf were computed by scaling data measured at lower dynamic pressures assuming spectral density proportional to q^2. It is clear from the results in Figure 24 that the HARPOON captive flight vibration levels are well below the applicable design criterion.

It should be mentioned here that the data presented in Figure 24 are for straight and level flight. No data for sharp turns are available at the forward hook location. However, referring back to Figure 18, vibration levels at the seeker location were greatly increased at frequencies below 200 Hz by a high g turn maneuver. It is likely that the vibration levels at the forward hook would also be greatly increased at these low frequencies, perhaps to levels in excess of the design criterion at the very lowest frequencies (below 30 Hz.).

7.3 Captive Flight Surface Pressure Environment

The fluctuating pressure environment acting on the exterior

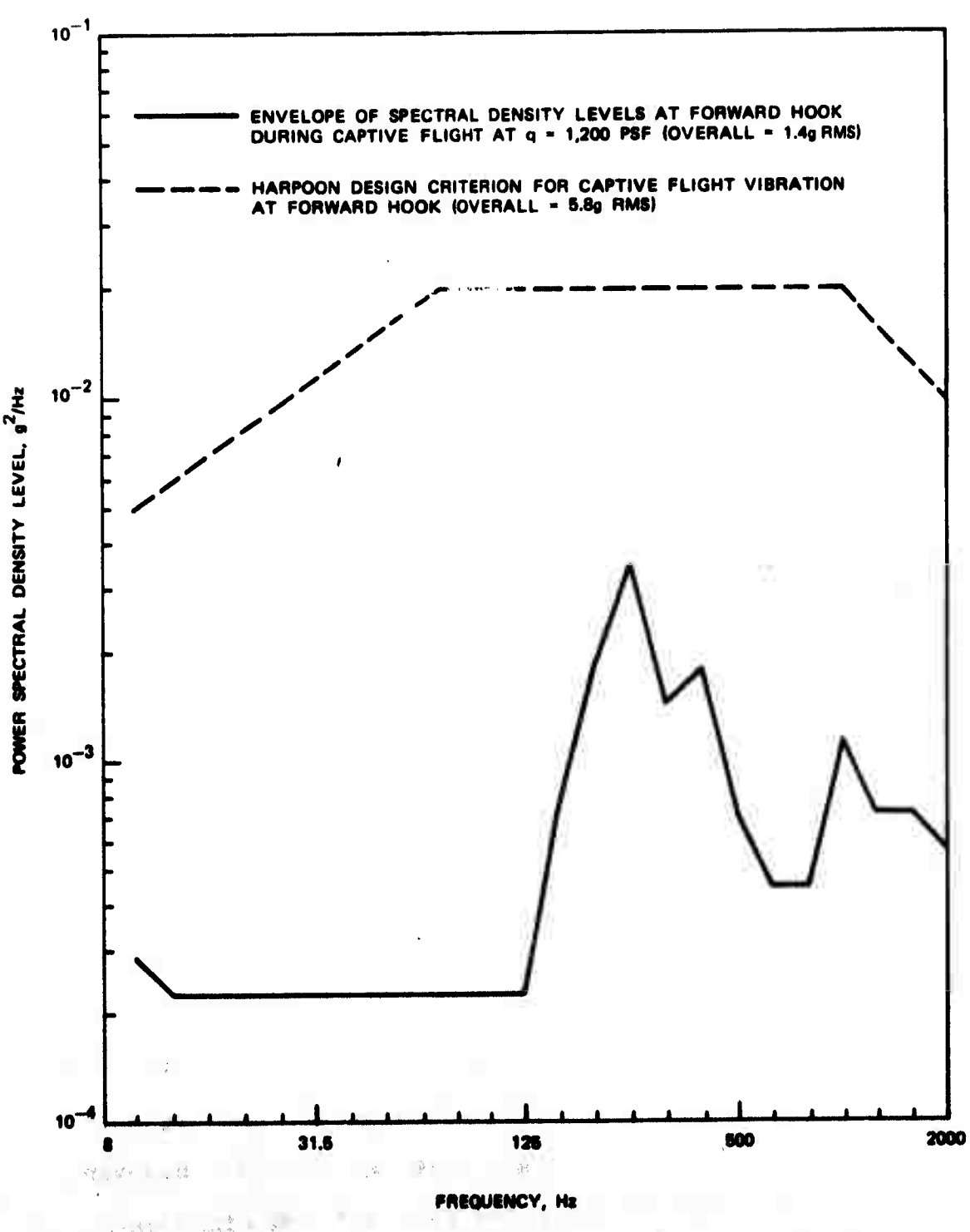

FIGURE 24. Comparisons of Captive Flight Vibration Levels to HARPOON Environmental Design Criterion.

surfaces of the HARPOON missile during captive flight is of two sources; (a) the aerodynamic noise which is most severe during flight at high dynamic pressures, and (b) the jet engine acoustic noise which is most severe during take-off. As noted in the previous section, the highest flight dynamic pressure anticipated for the aircraft involved in these experiments is estimated to be about 1200 psf for the A-7C aircraft. On the other hand, the worst case take-off noise occurs on the S-3A at locations on the missile facing the engine (location VV 14). These maximum fluctuating pressures and acoustic noise levels are shown in Figure 25. Note that the A-7C fluctuating pressure levels at the flight dynamic pressure of q = 1200 psf were computed by scaling data measurements at lower dynamic pressures assuming dB = C + 20 log q. Also shown in Figure 25 is the external acoustic noise design criterion for the HARPOON missile [2]. In all cases, the octave band levels are terminated at the 2,000 Hz center frequency because no measurements were obtained above this frequency.

The results in Figure 25 reveal that the overall pressure levels for the worst case captive flight conditions are well below the design criterion overall level of 165 dB. However, the octave band levels for both the take-off and high dynamic

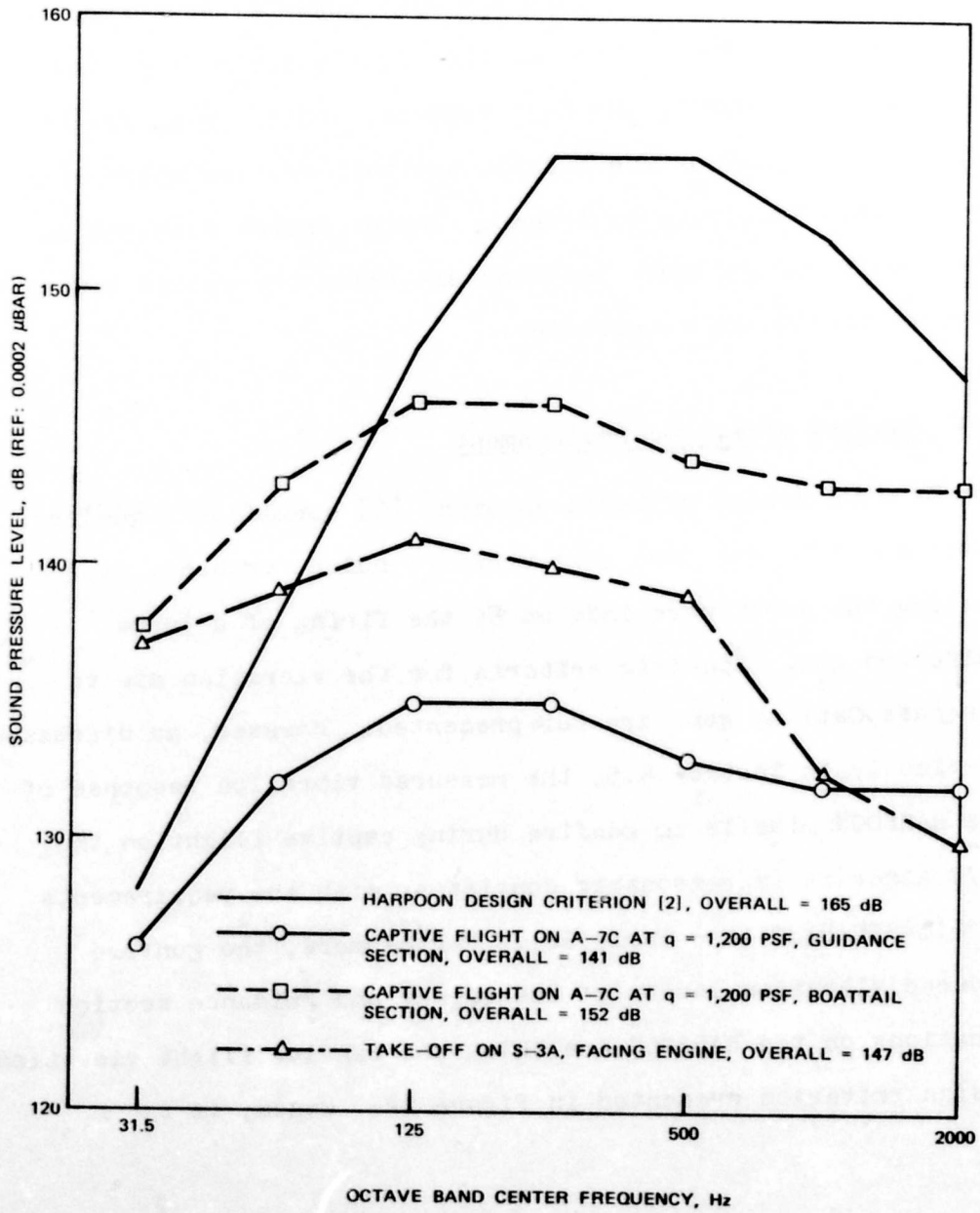

FIGURE 25. Comparisons of Exterior Fluctuating Pressure Levels to HARPOON Environmental Design Criterion.

pressure flight conditions do exceed the design criterion levels at frequencies below 100 Hz. These exceedances are not considered critical since the high take-off levels occur only over that limited area of the missile facing the wing mounted engine during the S-3A takeoff, and the high flight levels occur only on the missile boattail section which does not contain sensitive equipment. The pressures measured on the seeker and guidance sections are below the design levels even at the lowest frequencies.

7.4 Gunfire Vibration Environment

The HARPOON design criteria document [2] specifies a gunfire environment in the form of a pressure pulse, probably representing the shock wave induced by the firing of a large shipboard gun. Specific criteria for the vibration due to aircraft Gatling guns are not presented. However, as discussed previously in Section 6.5, the measured vibration response of the HARPOON missile to gunfire during captive flight on the A-7C aircraft is reasonably consistent with the requirements of MIL-STD-810C (see Table 12). Furthermore, the gunfire induced vibration levels at the seeker and guidance section locations on the HARPOON are below the captive flight vibration design criterion presented in Figure 24. Hence, it is

reasonable to assume that the missile is adequately designed for aircraft gunfire induced loads.

8. CONCLUSIONS

The principal conclusions to be drawn from the studies reported herein may be summarized as follows:

8.1 Catapult Launch Environment

The following conclusions apply to the shock response of the HARPOON missile mounted on weapons station No. 1 of an A-7E aircraft during catapult launches using a C-7 catapult.

(a) The maximum acceleration response of the missile occurs in the vertical direction at the forward end (the seeker), and is about 6 g peak.

(b) The Q = 10 shock spectra of the response levels at all locations are generally less than 10 g over the frequency range from 2.5 to 2000 Hz.

(c) The response levels are not significantly influenced by an off center position on the catapult or small variations in the launch speed.

(d) The response levels exceed, in some cases, the HARPOON design criterion for catapult launch loads, but are well within the design criteria for carrier handling and launch ejection shock loads.

8.2 Arrested Landing Environment

The following conclusions apply to the shock response of the HARPOON missile mounted on weapons station No. 1 of an A-7E aircraft during arrested landings using a MK-7 MOD 3 arresting gear.

(a) The maximum acceleration response of the missile occurs in the axial and vertical directions at the forward end (the seeker and guidance sections), and is about 4 g peak.

(b) The Q = 10 shock spectra of the response levels are generally less than 10 g at the forward hook over the frequency range from 2.5 to 2000 Hz, but reach values of about 50 g in the guidance section at frequencies above 1000 Hz.

(c) The response levels are not significantly influenced by the aircraft pre-landing sink rate or the landing speed.

(d) The response levels slightly exceed, in some cases, the HARPOON design criterion for arrested landing loads, but are well within the design criteria for carrier handling and launch ejection shock loads.

8.3 Captive Flight Vibration Environment

The following conclusions apply to the vibration levels of the HARPOON missile during captive flight on the P-3C, S-3A, and A-7C aircraft.

(a) The rms vibration levels at all locations are approximately proportional to flight dynamic pressure.

(b) The vibration levels during high dynamic pressure flight exceed the take-off vibration levels in most cases.

(c) The vibration levels during captive flight are relatively independent of the missile mounting location.

(d) For the same flight dynamic pressure, the spectral density levels of the vibration are similar in the frequency range above 200 Hz during captive flight on

all three aircraft tested. Below 200 Hz, the spectral levels during captive flight on the P-3C and S-3A aircraft are higher than on the A-7C aircraft, reflecting the difference in engine noise contributions among the three aircraft.

(e) The vibration levels in the frequency range below 200 Hz are significantly increased by sharp turns of the carriage aircraft.

(f) The vibration levels are substantially higher in the aft end of the missile than in the forward end.

(g) The maximum vibration levels at the forward hook location during straight and level flight are well below the HARPOON design criterion, which applies to this location.

8.4 Captive Flight Surface Pressure Environment

The following conclusions apply to the fluctuating pressures on the HARPOON missile exterior due to jet noise during take-off and aerodynamic noise during captive flight on the P-3C, S-3A, and A-7C aircraft.

(a) The rms fluctuating pressure levels on the missile exterior during captive flight are approximately proportional to flight dynamic pressure.

(b) The pressure levels during high dynamic pressure flight generally exceed the take-off levels, except for the S-A3 aircraft with the missile mounted on a weapons station adjacent to the wing mounted engine.

(c) The pressure levels during captive flight are relatively independent of the missile mounting location.

(d) The pressure levels during both take-off and high dynamic pressure captive flight are within the HARPOON design criterion acoustic levels at frequencies above 100 Hz. Below 100 Hz, the design criterion levels are exceeded at certain locations on the missile, but not over the entire missile as a whole.

8.5 Gunfire Vibration Environment

The following conclusions apply to the vibration levels of the HARPOON missile during captive flight on the A-7C aircraft with an M61A1 20 mm Gatling gun operating.

(a) The gunfire increases the rms vibration levels on the HARPOON structure by up to 100% over the normal levels during captive flight at a dynamic pressure of 700 psf.

(b) The gunfire increases the spectral levels of the vibration over a wide frequency range, although the greatest increase occurs at the gun firing rate frequency.

(c) There is no specific HARPOON design criterion for gunfire vibration, but the measured levels are broadly consistent with the test requirements of the proposed MIL-STD-810C.

REFERENCES

1. Piersol, A. G., "Evaluation of the HARPOON Missile Shock Environment During Ejection Launch by Aircraft Launchers," NWC TP 5881, Naval Weapons Center, China Lake, California, 1976.

2. "Environmental Design Criteria For The AGM-84A/RGM-84A Missile (HARPOON)," XAS-2381A, Naval Air Systems Command, Washington, D.C., 1972.

3. Rubin, S., "Concepts of Shock Data Analysis," Chapter 24, Shock and Vibration Handbook (Edited by C. M. Harris and C. E. Crede), Vol. 2, Mc Graw-Hill Book Company, Inc., New York, 1961.

4. Kelly, R.D., and Richman, G., Principles and Techniques of Shock Data Analysis, SVM-5, Shock and Vibration Information Center (DOD), Washington, D.C., 1969.

5. Bendat, J.S., and Piersol, A.G., Random Data: Analysis and Measurement Procedures, Wiley-Interscience, New York, 1971.

6. Crandall, S. H., and Mark, W. D., Random Vibration In Mechanical Systems, Academic Press, New York, 1963.

7. Piersol, A. G., "Vibration and Acoustic Test Criteria For Captive Flight of Externally Carried Aircraft Stores," AFFDL-TR-71-158, Wright-Patterson Air Force Base, Ohio, 1971.

8. Piersol, A. G., and Calkins, J. C., "Sparrow Missile Captive Flight: Simulation of Dynamic Loads," TP-73-35, Naval Missile Center, Point Mugu, California, 1973.

9. "Airborne Stores and Associated Suspension Equipment; General Design Criteria For," MIL-A-8591D, Department of Defense, Washington, D. C., 1968.

10. "Environmental Test Methods," MIL-STD-810C (Proposed), Aeronautical Systems Command, Wright-Patterson AFB, Ohio, 1974.

INITIAL DISTRIBUTION

27 Naval Air Systems Command
- AIR-03P (1)
- AIR-30212 (2)
- AIR-320 (1)
- AIR-330D (1)
- AIR-350 (1)
- AIR-5108C (1)
- AIR-5108C1 (1)
- AIR-5109B (1)
- AIR-5109B1 (1)
- AIR-5109E (5)
- AIR-5205 (1)
- AIR-53232 (1)
- AIR-53321 (1)
- AIR-5336 (1)
- AIR-5351 (1)
- AIR-5366 (1)
- AIR-53662 (1)
- AIR-53663 (1)
- AIR-53664 (1)
- AIR-954 (2)
- PMA-258 (1)

2 Chief of Naval Operations
- OP-703 (1)
- OP-722C (1)

1 Chief of Naval Material (MAT-0325B)

6 Naval Sea Systems Command
- SEA-0331 (1)
- SEA-0332 (1)
- SEA-09G32 (2)
- SEA-55211B (1)
- SEA-93 (1)

3 Naval Air Development Center, Johnsville
- Code AEHE, F. Smith (1)
- Code AM. J. Seidel (1)
- Technical Library (1)

2 Naval Air Engineering Center, Lakehurst (WESCO. C. R. Osmanski)

2 Naval Avionics Facility, Indianapolis
- Code ESS, H. Stone (1)
- Technical Library (1)

3 Naval Ordnance Station, Indian Head
- Code 3012A1, B. Boudreaux (1)
- Code REBO (1)
- Technical Library (1)

2 Naval Postgraduate School, Monterey
- R. E. Ball (1)
- L. V. Schmidt (1)

1 Naval Research Laboratory (Technical Library)
1 Naval Ship Missile Systems Engineering Station, Port Hueneme
4 Naval Surface Weapons Center, Dahlgren Laboratory, Dahlgren
  Code FVR, R. Hudson (1)
  Code TI, J. E. Hurtt (1)
  Code WXA, S. H. McElroy (1)
  Technical Library (1)
3 Naval Surface Weapons Center, White Oak
  Jack Gott (1)
  Vic Yarow (1)
  Technical Library (1)
1 Naval Undersea Center, San Diego
2 Naval Weapons Support Center, Crane
  Code RD (1)
  Cal Austin (1)
9 Pacific Missile Test Center, Point Mugu
  Code 5330 (1)
  Code 5333, C. V. Ryden (1)
  Code 5334, Bob Cannon (1)
  Code 5700, H. Harrison (1)
  A. A. Anderson (1)
  F. J. Brennan (1)
  Technical Library (1)
2 Office Chief of Research and Development
  Col. A Quinnelly (1)
  Technical Library (1)
2 Army Materiel Development and Readiness Command
  AMCRD-TV, Navakin (1)
  Technical Library (1)
1 Aberdeen Proving Ground (Technical Library)
4 Army Engineer Topographic Laboratories, Fort Belvoir
  GS-EC, Brierly (3)
  Technical Library (1)
2 Frankford Arsenal
  K-3400, D. Askin (1)
  Technical Library (1)
1 Harry Diamond Laboratories (Technical Library)
1 Picatinny Arsenal (Technical Library)
1 Headquarters, U.S. Air Force (Deputy Chief of Staff, Research and Development)
1 Air Force Armament Laboratory, Eglin Air Force Base
5 Air Force Rocket Propulsion Laboratory, Edwards Air Force Base
  Plans and Program Office (1)
  RPMCP (1)
  L. Meyer (1)
  Technical Library (1)
2 Armament Development and Test Center, Eglin Air Force Base
  R. Greene (1)
  Technical Library (1)

2 Directorate of Armament Development, Eglin Air Force Base
  Technical Library (1)
3 Wright-Patterson Air Force Base
  AFAL, AFSC (1)
  Charles Thomas (1)
  William Savage (1)
12 Defense Documentation Center
2 Applied Physics Laboratory, JHU, Laurel, MD
  Bill Caywood (1)
1 Bird Engineering Research Associate, Inc., Vienna, VA
1 Convair Division of General Dynamics, San Diego, CA
  (R. G. Huntington)
4 General Dynamics Corporation, Pomona Division, Pomona, CA
  Code 6-42, H. B. Godwin (1)
  Code 8-101, R. J. Carey (1)
  D. Underhill (1)
  Technical Library (1)
1 Honeywell, Inc., Systems and Research Division, Minneapolis, MN
  (J. D. Brennan)
1 Hughes Aircraft Company, Canoga Park, CA (R. J. Oedy)
1 Lockhead-California Company, Burbank, CA (Code 01 10, W. Hawkins)
4 Lockhead Propulsion Company, Redlands, CA
  C. J. Barr (1)
  W. A. Stevenson (1)
  Engineering Research, John H. Bonin (1)
  Technical Library (1)
11 McDonnell Douglas Corporation, St. Louis, MO
  J. H. Bell (9)
  J. L. Gubser (1)
  Technical Library (1)
2 Martin Company, Denver, CO
  F. A. Thompson (1)
  Technical Library (1)
1 Raytheon Company, Waltham, MA. (D. H. Sanders)
2 Rocketdyne, McGregor, TX
  Sparrow/Shrike Project Manager (1)
  Technical Library (1)
2 Sandia Corporation, Albuquerque, NM
  J. Foley (1)
  Technical Library (1)
1 Sandia Corporation, Livermore, CA (Technical Library)
2 Teledyne, CAE, Toledo, OH
  Harpoon Office (1)
  Technical Library (1)
1 Texas Instruments, Inc., Dallas, TX. (Missile & Ordnance Division,
  J. E. Tepera)
3 The Martin Company, Orlando, FL
  Code 143, J. A. Roy (1)
  P. G. Hahn (1)
  Technical Library (1)

1 Thiokol Chemical Corporation, Wasatch Division, Brigham City, UT
(R. Brown)
2 Value Engineering Company, Alexandria, VA
John Toomey (1)
Technical Library (1)